HHS Public Access

Author manuscript

Sci Immunol. Author manuscript; available in PMC 2023 May 15.

Published in final edited form as:

Sci Immunol. 2022 October 21; 7(76): eabo3420. doi:10.1126/sciimmunol.abo3420.

Depletion of exhausted alloreactive T cells enables targeting of stem-like memory T cells to generate tumor-specific immunity

Simone A. Minnie[1], **Olivia G. Waltner**[1], **Kathleen S. Ensbey**[1], **Nicole S. Nemychenkov**[1], **Christine R. Schmidt**[1], **Shruti S. Bhise**[1], **Samuel RW. Legg**[1], **Gabriela Campoy**[1], **Luke D. Samson**[1], **Rachel D. Kuns**[2], **Ting Zhou**[3], **John D. Huck**[3], **Slavica Vuckovic**[2], **Danniel Zamora**[4,8], **Albert Yeh**[1,4], **Andrew Spencer**[5,6,7], **Motoko Koyama**[1], **Kate A. Markey**[1,4], **Steven W. Lane**[2], **Michael Boeckh**[1,4,8], **Aaron M. Ring**[3], **Scott N. Furlan**[1,9], **Geoffrey R. Hill**[1,4]

[1]Clinical Research Division, Fred Hutchinson Cancer Center; Seattle, WA, 98109, UNITED STATES.

[2]QIMR Berghofer Medical Research Institute; Brisbane, QLD, 4006, AUSTRALIA.

[3]Department of Immunobiology, Yale School of Medicine; New Haven, CT, 06519, UNITED STATES.

[4]Department of Medicine, University of Washington; Seattle, WA, 98109, UNITED STATES.

[5]Australian Center for Blood Diseases, Monash University/The Alfred Hospital; Melbourne, VIC, 3004, AUSTRALIA.

[6]Malignant Haematology and Stem Cell Transplantation, The Alfred Hospital; Melbourne, VIC, 3004, AUSTRALIA.

[7]Department of Clinical Haematology, Monash University; Melbourne, VIC, 3800, AUSTRALIA.

[8]Vaccine and Infectious Disease Division, Fred Hutchinson Cancer Center; Seattle, WA, 98109, UNITED STATES.

[9]Department of Pediatrics, University of Washington; WA, 98105, UNITED STATES.

Abstract

Some hematological malignancies such as multiple myeloma are inherently resistant to immune-mediated anti-tumor responses, the cause of which remains unknown. Allogeneic bone marrow transplantation (alloBMT) is the only curative immunotherapy for hematological malignancies due to profound graft-versus-tumor (GVT) effects but relapse remains the major cause of death. We developed murine models of alloBMT where the hematological malignancy is either sensitive (acute myeloid leukemia [AML]) or resistant (myeloma) to GVT effects. We found that $CD8^+$ T cell exhaustion in bone marrow was primarily alloantigen-driven, with expression of

Corresponding Author: Prof. Geoffrey R. Hill, Fred Hutchinson Cancer Research Center, 1100 Fairview Ave N, Seattle, WA98109, USA, Ph 206 667 3324, grhill@fredhutch.org.

Authorship contributions: SAM designed and performed experiments, analyzed data and wrote the manuscript. OGW analyzed data. NN, KSE, CRS, GC, SSB, SL, LS and RDK performed experiments. KAM, MK, AY and SV assisted with data interpretation and experimental design. TZ, JDH, SWL, DZ, AS, MB, AMR provided reagents and/or interpreted data. SNF analyzed and interpreted data. GRH conceived the study and wrote the manuscript. All authors edited and approved the final manuscript.

Competing interests: All other authors declare that they have no competing interests.

inhibitory ligands present on myeloma but not AML. Due to this tumor-independent exhaustion signature, immune checkpoint inhibition (ICI) in myeloma exacerbated graft-versus-host disease (GVHD) without promoting GVT effects. Administration of post-transplant cyclophosphamide (PT-Cy) depleted donor T cells with an exhausted phenotype and spared T cells displaying a stem-like memory phenotype with chromatin accessibility present in cytokine signaling genes including the IL-18 receptor. While ICI with anti-PD-1 or anti-TIM-3 remained ineffective after PT-Cy, administration of a decoy-resistant IL-18 (DR-18) strongly enhanced GVT effects in both myeloma and leukemia models, without exacerbation of GVHD. We thus defined mechanisms of resistance to T cell-mediated anti-tumor effects after alloBMT and described an immunotherapy approach targeting stem-like memory T cells to enhance anti-tumor immunity.

One Sentence Summary:

Expansion of stem-like memory T cells after depletion of exhausted alloreactive T cells enhances graft-versus-tumor effects.

Introduction

T cell exhaustion is a well described driver of loss of immunosurveillance in many cancers, including hematological malignancies (1–4). The use of immunotherapies, such as immune checkpoint inhibition (ICI), has been a successful strategy to enhance anti-tumor effects in solid tumor settings as well as selected hematological malignancies (5–7). The importance of precursor exhausted and stem-like memory T cell subsets in generating a sustainable response to immunotherapies is becoming increasingly recognized, which has generated interest in targeting these populations directly (8–10). In hematological malignancies, particularly leukemias, allogeneic stem cell transplantation (alloBMT) remains the only curative immunotherapy option (11). The curative potential of BMT is largely mediated by donor T cells recognizing recipient alloantigen comprising hematopoietic or tumor-specific antigens on the underlying malignancy, which is referred to as the graft-versus-tumor (GVT) effect (12). However, alloBMT is limited by donor T cell recognition of alloantigen on normal tissue, a process known as graft-versus-host-disease (GVHD), as well as relapse of the original malignancy attributable to immune escape (13).

Studies where patients received PD-1 blockade after alloBMT have been associated with the exacerbation of GVHD, consistent with the role of PD-1 in suppressing alloreactive donor T cell function (14, 15). While there are a number of described mechanisms for immune escape after alloBMT (16), some hematological malignancies (e.g. myeloma (13, 17)) are inherently resistant to graft-versus-tumor responses and the cause of this remains unknown. Importantly, eliciting a strong GVT effect without inducing lethal GVHD likely requires modulation of the T cell repertoire such that highly alloreactive T cells are eliminated prior to initiating immunotherapy and/or immunotherapy selectively targeting tumor-specific T cells.

In this study, we first sought to understand why some hematological malignancies are resistant to GVT effects by developing pre-clinical models that were sensitive (acute myeloid leukemia [AML]) or resistant (myeloma) to GVT after alloBMT. Secondly, we

utilized multiome single cell sequencing techniques to phenotype T cells in the bone marrow microenvironment and identify pathways that could be targeted to improve GVT effects after alloBMT. We observed broad, alloantigen-induced $CD8^+$ T cell exhaustion that could be reduced with an immune suppressant routinely utilized after alloBMT, cyclophosphamide (PT-Cy), which shifted the induction of $CD8^+$ T cell exhaustion to a malignancy-driven phenotype at myeloma relapse. Multiome sequencing demonstrated increased chromatin accessibility and RNA expression of the IL-18 receptor on stem-like memory $CD8^+$ T cells after PT-Cy. Finally, we tested several immunotherapies after PT-Cy and found that while ICI did not induce lethal GVHD it also failed to enhance GVT effects. Conversely, an IL-18 cytokine mimetic (DR-18) facilitated potent anti-tumor responses in both myeloma and leukemia without markedly exacerbating GVHD.

Results

Graft-versus-myeloma effects are subverted after alloBMT

To determine potential factors underlying the resistance of patients with myeloma to graft-versus-tumor effects, we generated preclinical murine models of transplantation for primary AML and myeloma that we found to be GVT-sensitive and GVT-resistant, respectively. To achieve this, we developed a system of allogeneic BMT where C57Bl/6 recipients are transplanted with bone marrow (BM) and T cell grafts from minor-MHC mismatched C3H.SW donors (alloBMT) or syngeneic C57Bl/6 donors (synBMT). We utilized a GFP-expressing MLL-AF9-driven leukemia that allows for monitoring of tumor cells in peripheral blood and Vk*MYC myeloma that secretes IgG, which can be monitored by serum protein electrophoresis as an M-band (albumin/gamma ratio) which is a hallmark of clinical disease. In mice bearing MLL-AF9-driven AML, recipients of allogeneic grafts had significantly reduced circulating leukemia cells and a reduced relapse-related mortality compared to synBMT, confirming an allogeneic graft-versus-leukemia (GVL) effect (Figure 1A–B). Mice with late leukemia-related deaths in the alloBMT group succumbed to marrow failure, consistent with systemic immune control but local escape from GVL effects in the BM. In contrast, ineffective graft-versus-myeloma (GVM) responses were seen in Vk*MYC myeloma-bearing recipients with no significant difference in the rate of myeloma growth as determined by M-band progression. Furthermore, competing risk analysis revealed that there was a significantly increased risk of GVHD in alloBMT recipients compared with synBMT that outweighed any potential GVM effects (Figure 1C–D). Thus although an effective GVT response could be generated after alloBMT against AML, this was subverted in MM-bearing recipients; an observation which recapitulates clinical data demonstrating that myeloma is largely resistant to GVT effects (17). Importantly, mechanisms underpinning this GVT resistance could be broadly applicable clinically, as some patients with AML have reduced GVT sensitivity relative to highly sensitive malignancies (e.g. chronic myeloid leukemia) (18).

Donor $CD8^+$ T cells undergo exhaustion in response to allogeneic rather than tumor antigens after alloBMT

To determine the mechanisms responsible for the ineffective GVM response after alloBMT, we performed immune phenotyping of $CD8^+$ T cells in the BM between 2 and 8 weeks after

transplantation using flow cytometry. These experiments were performed in the absence of myeloma (MM-free) to control for the effects of concurrent myeloma on $CD8^+$ T cell function after BMT (3). We focused on $CD8^+$ T cells initially since GVHD in this model is primarily MHC class I-dependent and we have previously shown that $CD8^+$ T cells are crucial to long-term myeloma-specific immunity after autologous BMT (19). We used multidimensional t-SNE analysis of our flow cytometry data and observed differential clustering of allogeneic and syngeneic $CD8^+$ T cells by 2 weeks after transplant (Figure 2A). This phenotype persisted through to 8 weeks after transplant. We noted a significant expansion of $CD8^+$ T cells 2–4 weeks after transplant in alloBMT recipients which were predominately effector memory T cells ($CD44^+CD62L^-$, T_{EM}; Figure 2B–C). Conversely, synBMT recipients had equivalent $CD4^+$ and $CD8^+$ T cell expansion with higher frequencies of central memory ($CD44^+CD62L^+$, T_{CM}) versus T_{EM} $CD8^+$ T cells (Figure 2 B–C). Strikingly, the majority of $CD8^+$ T cells expressed TIGIT, PD-1 and TIM-3 early after alloBMT, and both PD-1 and TIGIT expression persisted long term (Figure 2D). DNAM-1 expression was maintained on a proportion of $CD8^+$ T cells after alloBMT, suggesting that these T cells were either activated or at an early stage of exhaustion (Figure 2A) (3, 20). Expansion of these alloreactive $CD8^+$ T_{EM} cells after alloBMT would be expected to result in enhanced tumor control relative to synBMT, but this was only seen in response to AML, suggesting the subversion of GVM may reflect tumor-related differences, either intrinsic to myeloma or related to differential effects exerted by myeloma (versus AML) on the tumor microenvironment (TME). We therefore investigated the expression of relevant inhibitory receptor ligands on the cell surface of Vk12653 myeloma and MLL-AF9 AML. We noted differential expression of both CD155 and PD-L1, the ligands for TIGIT and PD-1 respectively, on VK*MYC compared to MLL-AF9 (Figure 2E). This expression of CD155 on malignant cells has previously been demonstrated to infer resistance to T cell-dependent anti-tumor immunity (21). Furthermore, TIGIT has a much higher affinity than DNAM-1 for CD155 and will outcompete for ligand binding even if DNAM-1 expression is maintained on $CD8^+$ T cells (22). Therefore, donor $CD8^+$ T cells expressing high levels of $TIGIT^+$ and $PD\text{-}1^+$ in response to alloantigen were putatively inactivated via interaction with cognate inhibitory receptor ligands expressed by myeloma.

TIGIT inhibition does not enhance GVM after alloBMT

As CD155 and PD-L1 expression on myeloma cells is a potential mechanism of immune escape after alloBMT, we explored whether these pathways could be targeted therapeutically to generate GVM effects. Importantly, we have previously demonstrated that PD-1 or TIGIT blockade after synBMT significantly improved myeloma-specific immunity (3). PD-1 inhibition after alloBMT can exacerbate GVHD in both preclinical models and clinical practice (15, 23–25). To examine whether TIGIT inhibition would impact GVHD and/or GVM, we treated MM-bearing recipients with TIGIT blocking antibodies. Recipients treated with an Fc-enabled (i.e. live) 4B1-G2a clone, αTIGIT-G2a, after transplant had significantly enhanced mortality compared to isotype control (cIg)-treated mice (Figure 2F). This was associated with an increase in GVHD clinical scores and GVHD-induced mortality, without an associated improvement in the GVM effect (Figure 2G–I).

We next tested the Fc-dead anti-TIGIT G1-D265A clone (αTIGIT-G1) that does not deplete TIGIT-expressing regulatory T cells and hypothesized that exacerbation of GVHD would be less severe than the Fc-enabled TIGIT (26, 27). Indeed, mice treated with αTIGIT-G1 from 3 weeks after alloBMT had similar overall survival compared to isotype treated mice (Figure S1A). GVHD, myeloma burden, and myeloma progression were similar between αTIGIT-G1 and cIg-treated mice (Figure S1B–D). Therefore, TIGIT inhibition was not sufficient to generate GVM responses after alloBMT. This is in contrast to previous data demonstrating that blockade of myeloma-induced TIGIT expression on $CD8^+$ T cells could induce potent myeloma immunity in a synBMT model (where alloantigen is absent) (3). This led us to investigate whether the expression of inhibitory receptors on $CD8^+$ T cells was generated by $CD8^+$ T cell recognition of malignancy-derived antigens or broadly by recipient alloantigens after alloBMT.

Myeloma itself does not drive T cell exhaustion after alloBMT

In order to determine the relative contribution of tumor versus allogeneic antigens to $CD8^+$ T cell exhaustion we analyzed $CD8^+$ T cells in the BM of myeloma-bearing recipients (MM-bearing) or control mice that were transplanted in the absence of myeloma (MM-free) at 8 weeks after alloBMT, a timepoint of active myeloma progression in the MM-bearing cohort. We noted only a small increase in PD-1 and TIM-3 expression and reduced DNAM-1 expression in MM-bearing versus MM-free controls (Figure 3A–B). In particular, an increase in the frequency of $CD101^+CD38^+CD8^+$ T cells was seen in MM-bearing compared to MM-free mice (Figure 3B); a phenotype that is usually associated with dysfunctional, terminally exhausted T cells (3, 28). Nonetheless, $CD8^+$ T cells from MM-bearing mice did not have alterations in IFNγ or TNF production upon ex vivo restimulation (with PMA/ionomycin) after alloBMT compared with MM-free mice (Figure 3C), likely due to the relatively low frequency of $CD38^+CD101^+$ cells within the $CD8^+$ T cell compartment. Together, these data demonstrate that cytokine production by BM $CD8^+$ T cells was not adversely affected by the presence of myeloma after alloBMT. Similar analyses in AML-bearing mice also demonstrated a significant increase in PD-1 expression and a concurrent decrease in DNAM-1 expression compared to AML-free mice (Figure 3D–E). However, in AML-bearing mice the overall frequency of $IFN\gamma^+$ $CD8^+$ T cells was reduced (Figure 3F), indicating that tumor-induced $CD8^+$ T cell dysfunction occurred in this leukemia model. The absence of exaggerated $CD8^+$ T cell exhaustion in mice with relapsed myeloma after alloBMT confirms that the main driver of T cell exhaustion in this setting is alloantigen rather than tumor-specific antigen; potentially explaining why TIGIT blockade exacerbated GVHD without promoting GVM (Figure 2F–I).

Post-transplant cyclophosphamide attenuates alloantigen-induced $CD8^+$ and $CD4^+$ T cell exhaustion in the BM after alloBMT

We next investigated whether we could eliminate highly activated, alloreactive T cells in order to preserve T cell subsets that could be safely harnessed to improve GVT responses in the BM after alloBMT. To achieve this, we treated alloBMT recipients with a currently utilized GVHD prophylaxis strategy, post-transplant cyclophosphamide (PT-Cy) that strongly attenuates alloreactive T cell responses and GVHD. We first assessed T cell phenotypes in the BM 14 days after transplantation in MM-free mice, in order to

generate a dataset that could be broadly interpreted, independent of specific tumor-induced phenotypes. We performed single cell sequencing on sorted T cells from BM with the 10x Genomics Multiome platform to measure concurrent changes in gene expression (RNAseq) and chromatin accessibility (ATACseq). Unsupervised clustering based on weighted nearest neighbor algorithms identified 8 clusters within $CD8^+$ (Figure S2) and 5 clusters within $CD4^+$ (Figure S3) T cells. Clusters were annotated based on all differentially expressed genes in each cluster (Data file S1 and Data file S2) and we have highlighted key genes associated with each cluster in $CD8^+$ (Figure 4A) and $CD4^+$ (Figure 4B) T cells.

In untreated alloBMT recipients, $CD8^+$ T cells highly expressed genes associated with T cell exhaustion while those in PT-Cy-treated alloBMT recipients had higher expression of stem-like memory gene signatures (Figure 4C and Figure S4) (9, 29). When T cells were unbiasedly clustered, the majority of $CD8^+$ T cells from PT-Cy-treated recipients were within a cluster (number 6), which included stem-like memory cells (T_{SCM}) characterized by *Bach2*, *Ly6a* (encoding sca-1), *Il7r, Il18r1*, *Cd226* and absence of *Pdcd1* (Figure 4A). These changes in gene expression were mirrored by changes in chromatin accessibility as we observed a similar skewing towards stem-like signatures measured by gene accessibility scores (Figure 4C). Taken together, these findings confirm a fundamental change in the phenotype of $CD8^+$ T cells surviving PT-Cy. Analogous to the $CD8^+$ T cell compartment, $CD4^+$ T cells from alloBMT recipients were enriched for the same exhaustion signature, while those in PT-Cy-treated recipients were largely enriched for a T_{SCM} signature (Figure 4D and Figure S5). Furthermore, chromVAR analysis highlighted motifs associated with exhaustion (i.e. NR4A1 (30), NFATC (31)) in T cells from control alloBMT recipients, while T cells from PT-Cy-treated alloBMT recipients had motifs associated with stemness (i.e. TCF7 (32), KLF) (Figure S6). To identify functional relevance of PT-Cy-driven epigenetic changes, we measured chromatin accessibility in key cytokine receptor genes and noted that *Il18r1* (IL-18R), *Il2ra* (IL-2Rα) and *Il7r* (IL-7R) demonstrated increased gene activity scores after PT-Cy in both $CD8^+$ and $CD4^+$ T cells (Figure 4E–F).

Finally, we corroborated our sequencing data of BM T cells from alloBMT recipients with and without PT-Cy with flow cytometry at the same timepoint, including synBMT recipients as a baseline for any immune effects of transplantation itself. We confirmed that $CD8^+$ T cells had an exhausted phenotype after alloBMT, characterized by expression of high levels of TIGIT, PD-1, TOX and TIM-3 proteins, while syngeneic T cells were DNAM-1^+ without inhibitory ligand expression (Figure 4G–H and Figure S7A). $CD8^+$ T cells from PT-Cy-treated alloBMT recipients had significantly increased DNAM-1 and reduced TIGIT, PD-1 and TOX expression, with a phenotype intermediate to T cells from alloBMT recipients without PT-Cy and recipients of synBMT (where alloantigen was absent). Interestingly, PT-Cy treatment did not abrogate granzyme B production by $CD8^+$ T cells, as determined by both RNA and protein expression (Figure S4 and S7A). The striking effect of PT-Cy on the $CD4^+$ T cell compartment was also by confirmed by flow cytometry such that the $CD4^+$ T cell exhaustion signature in $FoxP3^-$ conventional $CD4^+$ T cells from PT-Cy-treated recipients were largely indistinguishable from synBMT recipients, consistent with a dominant effect on class II-dependent alloreactivity (Figure 4I–J and Figure S7B). Together these data demonstrate that PT-Cy reduced the frequency of alloreactive, exhausted T cells

in the BM of alloBMT recipients, and instead enriched for T_{SCM} populations, offering a potential platform on which to subsequently generate tumor-specific responses.

PT-Cy is permissive of myeloma-driven T cell exhaustion after alloBMT

We next treated MM-bearing recipients with PT-Cy after alloBMT and compared myeloma growth and survival to untreated recipients to determine whether the loss of putative alloreactive T cells in the BM impacted the control of myeloma. PT-Cy resulted in early myeloma cytoreduction with reduced M-bands at 4 weeks after alloBMT that was also seen in recipients of T cell depleted BM (Figure 5A–B), consistent with the expected cytoreduction mediated by cyclophosphamide. However, this PT-Cy effect was not durable as there was a subsequent increase in myeloma progression as determined by M-band 8 weeks after alloBMT in PT-Cy-treated recipients (Figure 5A). Consistent with this effect, total T cell numbers were also concurrently reduced by PT-Cy at D+14 and D+21 after alloBMT (Figure S9A–B). Taken together, these data suggest that direct myeloma cytoreduction partially counteracts the loss of alloreactive T cells mediating graft-versus-tumor effects after PT-Cy.

Having established that PT-Cy reduced alloantigen-induced T cell exhaustion, enriched for a T_{SCM} phenotype, and did not significantly reduce overall survival, we next sought to determine whether the presence of myeloma in the BM would alter T cell phenotypes in PT-Cy-treated alloBMT recipients with relapsed disease. We analyzed $CD8^+$ and $CD4^+$ T cells at 7 weeks post-transplant, from the BM of MM-bearing and MM-free allograft recipients that were treated with and without PT-Cy. In untreated recipients, there was high expression of TIGIT, TIM-3 and TOX on $CD8^+$ T cells regardless of whether the mice were MM-free or had active myeloma, indicative of broad alloantigen-driven T cell exhaustion (Figure 5C, F–G). In MM-free PT-Cy-treated recipients, the majority of the $CD8^+$ T cells were DNAM-1^+TIGIT$^-$ and did not express TOX or TIM-3 (Figure 5C, F–G); consistent with maintained depletion of exhausted alloreactive T cells observed at D+14 (Figure 4). However, in MM-bearing PT-Cy-treated recipients, the majority of the $CD8^+$ T cells were DNAM-1^-TIGIT$^+$ with high expression of TOX and TIM-3 (Figure 5C, F–G); consistent with the onset of myeloma-driven T cell exhaustion. Notably, even at this late timepoint, the reduction in total numbers of $CD4^+$ and $CD8^+$ T cells in PT-Cy-treated recipients was maintained (Figure 5D). In PT-Cy-treated MM-free recipients, there was an increase in $CD8^+$ central memory (T_{CM}; $CD44^+CD62L^+$) and a decrease in terminal effector (T_{EFF}; $CD44^-CD62L^-$) T cells, consistent with maintenance of the memory populations we identified at earlier timepoints (Figure 4C and Figure 5E). Increased expression of TOX and inhibitory receptors, including the terminal exhaustion markers TIM-3 and CD101, on effector cells in MM-bearing compared with MM-free PT-Cy-treated recipients is consistent with the expansion of exhausted, putatively myeloma-specific T cells; a phenotype observed at MM progression after synBMT (3). Therefore, PT-Cy effectively eliminated alloantigen-driven $CD8^+$ T cell exhaustion and enabled exhaustion to instead be driven by myeloma. Although there was a marked effect on $CD4^+$ T cells after PT-Cy, there were only subtle differences in this compartment in MM-free versus MM-bearing recipients, including an increase in TOX but not TIGIT or TIM-3 expression (Figure 5C, H–I). This finding is unsurprising, given the high expression of MHC class I and absence of MHC class II on

Vk*MYC myeloma cells (19). Finally, we confirmed the presence of tumor-driven T cell exhaustion after PT-Cy in the MLL-AF9 AML model. We observed an increased frequency of TIM-3^{+}CX3CR1^{-} CD8^{+} T cells at 3 weeks post-transplant in mice with relapsed AML compared to AML-free recipients after PT-Cy (Figure S8). Expression of CX3CR1 was used to exclude transitionary effector cells that contaminate the TIM-3^{+} population at earlier timepoints in tumor progression (33).

Agonist immunotherapies are required to promote GVM after PT-Cy

Given the presence of myeloma-driven expression of inhibitory receptors on CD8^{+} T cells after PT-Cy relapse, we tested the anti-myeloma efficacy of immune checkpoint inhibition (ICI) in PT-Cy-treated alloBMT recipients (Figure 6A). We administered ICIs, either anti-PD-1 or anti-TIM-3, from D+7 for 4 weeks and observed no reduction in myeloma burden in ICI-treated mice (Figure 6B–C). For ICI to be effective, there must be an appropriate ratio of ICI-responsive T cells to tumor burden (34). Importantly, PT-Cy resulted in reduced expression of inhibitory receptors (Figure 4C) in the context of strongly reduced overall T cell numbers (Figure S9) at the timepoint where ICI was administered. These data suggest that immunotherapies targeting a ‘brake’ on T cell function were unlikely to drive effective anti-myeloma responses in this setting. To that end, we next investigated two immunotherapies with known direct agonist activity, decoy-resistant IL-18 (DR-18 (35)) and anti-CD137 (4–1BB (19)). DR-18 is a synthetic cytokine that is resistant to the IL-18 binding protein, which usually counteracts the pro-inflammatory effects of native IL-18 in vivo. In solid tumor models, DR-18 promotes IFNγ-dependent, CD8^{+} T cell-mediated anti-tumor responses (35). We were especially interested in this agonist as IL-18R gene expression and chromatic accessibility was increased in both CD4^{+} and CD8^{+} T_{SCM} cells (Figure 4A–B, E–F). Furthermore, IL-18R is known to be expressed on human memory T cells, and we have confirmed expression of IL-18R on CD4^{+} and CD8^{+} T_{SCM} in patients who underwent allogeneic stem cell transplantation (Figure S10) (36). The CD137 agonist was chosen due to known anti-myeloma activity in other preclinical models and CD137 (Tnfrsf9) was broadly expressed across CD8^{+} T cell clusters irrespective of PT-Cy treatment (Figure S3) (19, 37). When administered from 3 days after PT-Cy, both agonist immunotherapies promoted anti-myeloma responses, as evidenced by decreased M-bands at 4 and 6 weeks compared to PT-Cy alone (Figure 6D). Although GVHD clinical scores were minimally elevated in agonist-treated mice, they remained below those of alloBMT recipients without PT-Cy (Figure 6D), consistent with the absence of substantial GVHD.

We next investigated the mechanisms of action of DR-18 and anti-CD137 after PT-Cy. We observed a significant increase in the concentration of serum IFNγ and, to a lesser extent, TNF in DR-18- but not anti-CD137-treated recipients compared with PT-Cy alone (Figure 6E). We then tracked immune responses in individual mice over time using serial bone marrow aspirates. At four weeks after alloBMT, CD8^{+} T cells from PT-Cy-treated mice could be grouped into three populations: non-activated/bystander (DNAM-1^{+}TIGIT^{-} and CD39^{-}TIM3^{-}), activated/effector (DNAM-1^{+}TIGIT^{+} and CD39^{int}TIM3^{-}), and exhausted (DNAM-1^{-}TIGIT^{+} and CD39^{hi}TIM3^{+}) cells. Interestingly, DR-18 preferentially expanded the activated/effector T cell subset whereas anti-CD137 promoted the exhausted phenotype (Figure 6F); an outcome possibly driven by the stem-like properties of the CD8^{+} T cells

expressing IL-18R. NK cells were also expanded in DR-18-treated mice (Figure 6G). Importantly, there was an almost complete elimination of MM cells from the BM of recipients treated with DR-18 or anti-CD137 by 6 weeks after alloBMT (Figure 6H). At this 6-week timepoint, we also noted an expansion of $CD8^+$ and $CD4^+$ T cells in anti-CD137-treated mice in BM but not in blood (Figure 6I and Figure S11A). In DR-18-treated mice, there was no change in T cell numbers; however, the number of DNAM-1^+ and cytolytic NK cells was significantly increased specifically in the marrow but not in the blood (Figure 6 I–J and Figure S11A–B).

Unbiased clustering of $CD4^+$ and $CD8^+$ T cell flow cytometry data utilizing FlowSOM revealed differential relative expansion of several immune phenotypes across treatment groups (Figure 6 K–L) (38). Heatmaps depict mean fluorescence intensity (MFI) of each included marker across 12 populations within $CD4^+$ T cells (Figure S12A). In αCD137-treated mice, Treg frequency was reduced while exhausted and effector $CD4^+$ T cell subsets were increased compared with DR-18-treated and PT-Cy only recipients (Figure S12B). DR-18 treatment specifically expanded a $CD62L^-$ Treg population (Figure S12C), suggested to be less suppressive and highly activated (39), without expanding the overall frequency of Tregs compared to PT-Cy only recipients. In the $CD8^+$ T cell compartment, DR-18 promoted $CD8^+$ T cell activation with a relative enrichment in non-exhausted effector populations (Figure 6L and Figure S13) and increased frequency of DNAM-1^+TIGIT$^+$ and $CD39^{int}TIM3^-$ subsets (Figure 6M–N) compared to PT-Cy alone recipients. At this timepoint, $CD8^+$ T cells from αCD137-treated recipients were largely terminally exhausted (Figure 6 L–N) although the total number of cytotoxic granzyme B^+ or perforin$^+$ $CD8^+$ T cells was increased (Figure 6O–P). In the blood, DR-18 reduced the total number of $CD4^+$ and $CD8^+$ T cells, however treatment increased the frequency of T_{EM} in both compartments (Figure S11A, C–D). Treatment with αCD137 increased expression of granzyme B, PD-1, CD39 and TOX on $CD8^+$ T cells in the blood but not to the same extent as observed in the BM (Figure S11E). Therefore, agonist immunotherapy promoted immune cell activation, largely in the BM TME, and generated potent myeloma immunity after PT-Cy. Interestingly, DR-18 treatment generated a less terminally exhausted phenotype compared to anti-CD137, potentially due to the expression of IL-18R on stem-like $CD8^+$ and $CD4^+$ T cells after PT-Cy.

Decoy-resistant IL-18 promotes potent graft-versus-leukemia effects.

We next sought to explore the combination of agonist immunotherapy with PT-Cy in a model of haploidentical transplantation (haploBMT); a setting where PT-Cy is a clinical standard of care. In this model, there is a major genetic mismatch between the recipient and the donor whereby lethal GVHD occurs in the absence of any immunosuppressive interventions. Here we utilized a BCR-ABL-NUP98hox9 leukemia, which is GVL-sensitive (Figure 7A). In this model, untreated halpoBMT recipients developed lethal GVHD and although PT-Cy reduced the incidence of lethal GVHD, treatment increased relapse-related mortality such that there was no difference in overall survival (Figure 7B). DR-18 administration after PT-Cy significantly improved GVL responses and overall survival while CD137 agonism had no anti-tumor efficacy in this model (Figure 7B).

To explore the mechanisms of DR-18-driven GVL in a haploBMT setting, we utilized donor cells from a triple reporter mouse (FoxP3-RFP x IL-10-GFP x IFNγ-YFP) to measure in vivo cytokine production without re-stimulation. We performed phenotyping in mice with low leukemia burden to minimize the effect of tumor cells on T cell number in the BM. PT-Cy-treated recipients had reduced $CD8^+$ T cell numbers in the BM, but increased NK cells compared to untreated haploBMT recipients (Figure 7C). The frequency of $IFN\gamma^+$ $CD8^+$ T cells was minimally decreased after PT-Cy while $CD4^+$ IFNγ production was unaffected (Figure 7D). DR-18 did not alter IFNγ production from T cells after PT-Cy (Figure 7D) but did increase DNAM-1 expression (Figure 7E–F) and reduced TOX and TIM-3 expression (Figure 7G) on $CD8^+$ T cells. $CD8^+$ T cells from DR-18-treated recipients also had significantly increased granzyme B (GrzB) and granzyme A (GrzA) secretion compared to both untreated haploBMT recipients and PT-Cy alone (Figure 7H). Interestingly, DR-18 also increased the frequency of $IFN\gamma^-$producing and $GrzA^+GrzB^+$ NK cells compared to both PT-Cy alone and untreated haploBMT recipients (Figure 7I–J). Together, these data highlight the ability of DR-18 to drive potent GVL effects by reducing $CD8^+$ T cell exhaustion and expanding cytotoxic NK cells after haploBMT with PT-Cy.

Discussion

Allogeneic BMT is the only curative treatment for many hematological malignancies, however some malignancies, particularly myeloma, are inherently resistant to GVT effects. Here we developed murine models of alloBMT that recapitulate these clinical observations in order to uncover the immunological mechanisms therein. High expression of inhibitory receptors after alloBMT in the absence of tumor antigen, together with our observed lack of GVM but exacerbated GVHD after ICI, suggests that alloantigen primarily drives T cell exhaustion after alloBMT in myeloma. Upregulation of TIGIT and PD-1 on $CD8^+$ T cells after alloBMT presumably enhanced myeloma-mediated suppression of activated alloreactive T cells in a tumor-antigen independent manner, as both PD-L1 and CD155 were highly expressed on VK12653 but were largely absent on MLL-AF9-driven AML. The reduction in IFNγ production in $CD8^+$ T cells from mice with relapsed AML compared to AML-free mice suggests that these T cells were at a more terminal stage of dysfunction that was driven by tumor-antigen. Nonetheless, a previous study has shown that TIGIT inhibition did not enhance GVL in a preclinical AML model, although anti-PD-1 did provide some anti-tumor activity (40). Vk*MYC myeloma expresses clinically relevant inhibitory ligands as both CD155 and PD-L1 have been observed on malignant plasma cells in patients with myeloma (41–46). Furthermore, these ligands are expressed on AML cells in some patients and may also contribute to GVT resistance and/or immune escape across several hematological malignancies (47–49).

The interaction of inhibitory ligand with their coupled receptors on T cells inhibits T cell cytolytic activity, reduces effector cytokine production, limits proliferation, and results in T cell apoptosis (50, 51). Importantly, inhibitory receptors are also highly expressed on human $CD8^+$ T cells in patients receiving either matched or haploidentical donor grafts (52, 53). Patients with relapsed disease after matched alloBMT had increased expression of inhibitory receptors on BM $CD8^+$ T cells compared to those achieving a complete response (52, 54), whereas there was no effect of tumor relapse on T cell exhaustion in haploidentical alloBMT

recipients (52). These clinical observations corroborate our hypothesis that alloantigen is a key driver of T cell exhaustion after alloBMT. These effects make subtle changes in T cell exhaustion at relapse difficult to ascertain and examination of this will require longitudinal analysis of $CD8^+$ T cell subsets by single cell approaches in large prospective studies of PT-Cy versus standard immune suppression in patients who relapse versus those who do not. Together with our findings, these data suggest that subversion of alloreactive T cells by inhibitory ligand expression may be operative in hematological malignancies.

Alloantigen not only increased expression of inhibitory receptors by donor T cells, but also the expression of exhaustion-associated gene signatures, chromatin accessibility within exhaustion-associated genes, and exhaustion-associated motifs. PT-Cy reduced these exhaustion signatures in both $CD8^+$ and $CD4^+$ T cells and instead enriched for stem-like memory phenotypes and *Tcf7*-driven motifs. We propose that establishment of a myeloma-driven exhaustion phenotype at relapse enabled agonistic immunotherapy interventions capable of enhancing myeloma-specific immunity without driving the lethal GVHD (as seen after ICI in the absence of PT-Cy). The inability of ICI to drive myeloma immunity after PT-Cy is likely due to cytoreduction of T cells and/or the absence of inhibitory receptor expression on T_{SCM} cells that are specifically enriched after PT-Cy. T_{SCM} cells have been described in the peripheral blood of patients after PT-Cy and our data demonstrates that T_{SCM} reside in the BM and have high expression of the IL-18R (55, 56). Furthermore, we have demonstrated that human T_{SCM} express the IL-18R after alloBMT. DR-18 administration after PT-Cy may act directly on these T_{SCM} cells to promote myeloma immunity and IFNγ production. IFNγ secretion by donor $CD8^+$ T cells is inversely correlated with their ability to cause GVHD explaining the absence of lethal GVHD after DR-18 (57). The lack of ICI efficacy and the potent anti-tumor effects of DR-18 also reflects the need for agonists that act as an accelerator to drive T cell activation after PT-Cy rather than the need for antibodies that block immunological brakes, checkpoints, in cells that are putatively not highly activated at the time of immunotherapy.

The mechanisms of action of PT-Cy have been explored in other studies using very high donor T cell doses and variable but often lower cyclophosphamide doses than used in our studies and clinically (58, 59). These studies demonstrate donor T cell depletion with relative sparing of regulatory T cells. Whether alloreactive T cells are differentially depleted by PT-Cy is less clear with disparate results depending on the T cell dose and alloreactive T cell clone being tracked. Certainly, we have noted early and profound depletion of all donor T cells, including alloreactive clones, by PT-Cy. Likewise, the effect of PT-Cy on GVL, if any, is not clear in clinical studies where patients are transplanted with heterogenous malignancies and levels of measurable residual disease that limit the power to discriminate effects (60–63). Importantly, the number of T cells needed to mediate an effective GVL response is substantially lower than that required to mediate lethal GVHD and so T cell depletion in vivo by PT-Cy does not necessarily mitigate an effective GVL, although it is likely quantitatively modified. Notably, a recent study provides clinical support for our hypothesis that PT-Cy reduces alloantigen T cell exhaustion and instead facilitates tumor-driven T cell exhaustion. In this study, authors observed a broad reduction in T cell exhaustion signatures by GSEA analysis in patients treated with PT-Cy, which was then increased in patients that went on to relapse (64). In our study, we demonstrated that T cell

exhaustion only occurred in the presence of high myeloma burden in the BM after PT-Cy, despite the fact that alloantigen persists at this site indefinitely through residual recipient stromal cells (65). Together, these data strongly suggest that tumor antigen, rather than alloantigen, drives T cell exhaustion after PT-Cy however this hypothesis requires formal examination in subsequent studies.

Utilization of donor NK cells to enhance GVL is being increasingly studied, particularly in context of haploidentical transplantation where missing MHC class I and NK-sensitive AML represent favorable immunological contexts to exploit this effect (66, 67). This is particularly relevant for DR-18, since this cytokine had a stimulatory effect on NK cells, in addition to the effects on $CD8^+$ T cells both in our transplantation models and previously published solid tumor systems (35). We have not excluded this effect as a complimentary mechanism of anti-tumor activity, and it is highly likely that the combination of both T and NK cell-mediated GVL is operative. AML is particularly sensitive to NK cell-mediated killing and this may underlie the lack of efficacy of CD137 agonism in leukemia, as αCD137 did not elicit the same NK cell expansion and activation as was seen with DR-18.

In conclusion, we have identified a previously unappreciated mechanism of ineffective GVT after alloBMT whereby T cell exhaustion is driven primarily by alloantigen and exacerbation of GVHD does not confer enhanced GVM. Rather, the use of PT-Cy eliminated donor T cell exhaustion signatures and enriched for stem cell memory gene activity early post-alloBMT. This immunophenotype can be targeted with agonistic immunotherapy approaches to enhance GVM and GVL without exacerbating GVHD in both MHC-matched and haploidentical transplantation models. These data provide the rationale for investigation of the use of PT-Cy based immune suppression as a platform for subsequent agonist immunotherapies after allogenic stem cell transplantation. More broadly, our data demonstrate that stem-like memory T cells are more responsive to agonist immunotherapies than immune checkpoint inhibition and can be targeted by DR-18 to promote anti-tumor effects without driving terminal T cell exhaustion.

Materials and Methods

Study Design

This study was designed to interrogate mechanisms behind ineffective graft-versus-tumor (GVT) responses after allogeneic stem cell transplantation. We developed murine models that were sensitive or resistant to GVT effects and used flow cytometry alongside multiomic single cell RNA sequencing approaches to interrogate CD4 and CD8 T cell phenotypes in the bone marrow. We then used post-transplant cyclophosphamide and agonist immunotherapies to overcome GVT resistance and drive potent anti-tumor responses. Mice were randomly assigned to groups in all experiments without investigator blinding. All *n* values reflect biological replicates and numbers of mice per group are included, with the statistical test performed, in the caption for each figure.

Mice—Female C57BL/6 mice were purchased from the Animal Resources Centre (Perth, Western Australia, AUS) or Jackson Laboratory (Bar Harbor, ME, USA). C3H.SW mice were purchased from Jackson Laboratory and subsequently bred in house (QIMR Berghofer

Medical Research Institute, Brisbane, QLD, AUS; Fred Hutchinson Cancer Center, Seattle, WA, USA). Female B6D2F1 mice were purchased from Charles River and subsequently bred in house (Fred Hutchinson Cancer Center). FoxP3-RFP x IL-10-GFP x IFNγ-YFP mice were bred in house (Fred Hutchinson Cancer Center). Mice were housed in sterile microisolator cages and received acidified (pH 2.5), autoclaved water and normal chow. Mice were 8–12 weeks of age when used in experiments. All animal procedures were performed in accordance with protocols approved by the institutional animal ethics committee.

Stem cell transplantation—Recipient mice were injected intravenously with Vk12653, which originated from Vk*MYC transgenic mice (68, 69), two weeks prior to BMT (1×10^6 $CD138^+CD19^{neg}$ cells; MM-bearing mice) or with an MLL-AF9-driven acute myeloma leukemia (MLL-AF9; AML, 0.1×10^6·GFP^+) or BCR-ABL-NUP98hox9 (1.0×10^6·GFP^+) on D0 (AML-bearing mice) (70, 71). Recipients were transplanted as described previously with BM and T cell grafts (doses detailed in the Figure Legends) administered via tail vein injection the day after lethal irradiation (1000cGy, ^{137}Cs source) (72). Every two weeks, serum samples were collected from MM-bearing recipients and M-band was quantified as previously described using a Sebia Hydrasys serum protein electrophoresis system (HYDRASYS 2 Scan) (68). Leukemia cell number in blood was calculated weekly using flow cytometry to quantify GFP^+ cells in blood. Recipients were monitored daily, up to 120 days post-BMT, and sacrificed when hind limb paralysis occurred or clinical scores reached ≥6 (73). In competing risk analyses, deaths were attributed to myeloma if the M-band was above 0.28, a previously defined relapse threshold (19). In the leukemia models, leukemic death was defined by a white blood cell count above 50×10^6/ml or a GFP^+ leukemia frequency above 50% in blood or BM.

For some experiments, mice were treated with 100 μg anti-TIGIT mAb (4B1, Bristol Myers Squibb) or mouse IgG2a (anti-KLH) twice a week for 4 weeks from D+14 post-alloBMT. For other experiments, mice were treated with 100 μg Fc-dead anti-TIGIT mAb (D265A, Bristol Myers Squibb) or mouse IgG1 (anti-KLH.1) twice a week for 6 weeks from D+21 post-alloBMT. Cyclophosphamide (Fischer Scientific; 99.5%, MP Biomedicals™) was administered I.P at 50 mg/kg on D+3 and D+4 after alloBMT (PT-Cy). After PT-Cy, 100 μg of anti-TIM-3 mAb (RMT3–23, BioXcell), anti-PD-1 mAb (RMP1–14, BioXcell), or anti-CD137 (4–1BB, 3H3, BioXcell) and related isotypes were administered i.p twice a week while 8 μg DR-18 (described (35)) was administered s.c. twice a week from D+7 for 4 weeks. DR-18 was supplied by Simcha Therapeutics (New Haven, CT).

Cell preparation for flow cytometry—Recipient mice were sacrificed 2–8 weeks post-transplant and cells from BM or blood were harvested. For bone marrow aspirates, mice were anesthetized and treated with a local analgesic (0.5% lidocaine) followed by injection of 30 μL of PBS into the femur to allow up to 10 μL of marrow to be aspirated for FACS analysis. For surface marker phenotyping, isolated cells were incubated with Fc-block prior to staining with fluorescently tagged antibodies (listed in Table S1), on ice for 30 minutes. For intracellular staining, cells were surface-labelled, fixed and permeabilized (eBiosciences – Foxp3 Transcription Factor Staining Buffer Kit) prior to

intracellular staining at room temperature for 60 minutes. To measure cytokine production, cells were stimulated for 4 hours at 37°C with PMA (500 ng/mL) and ionomycin (50 ng/mL) (Sigma-Aldrich) with Brefeldin A (BioLegend). All samples were acquired on a BD LSR Fortessa (BD Biosciences) or BD FACSymphony A3 (BD Biosciences) and analyzed using FlowJo software (v10). tSNE analysis was performed using the FlowJo plugin with default settings on a concatenated sample with 3000 CD8 T cells per mouse. FlowSOM analysis was performed with 3000 – 4000 CD8 or CD4 T cells per mouse concatenated after downsampling (38).

Single cell RNA/ATAC sequencing—Naïve C57Bl/6 mice were transplanted with C3H.SW grafts and were untreated (alloBMT) or treated with 50 mg/kg PT-Cy on D+3 and D+4 (PT-Cy). Bone marrow was harvested from femurs (4 mice pooled per group) at D+14 after alloBMT and T cells were sort purified ($CD90.2^+CD4^+$ and $CD90.2^+CD8^+$) before nuclei preparation according to the 10x Genomics Multiome protocol (CG000365_DemonstratedProtocol_NucleiIsolation_ATAC_GEX_Sequencing_RevB.pdf). Nuclei (also herein referred to as cells) were captured and libraries were generated according to manufacturer's specifications. Libraries were sequenced using an Illumina NovaSeq 6000 targeting a depth of 25,000 reads per cell per library.

Single cell RNA/ATAC analysis—Reads were demultiplexed and processed using cellranger-arc v1.0.1 aligning reads to GENCODE vM23/Ensembl98. Peaks were called from each sample's fragment file (cellranger output) using MACS2(74) using the parameters '--nomodel --extsize 200 --shift −100'. Quantification of reads in MACS2 peaks were calculated and integrated with cellranger RNA output using Signac (75). Cells meeting the following criteria (calculated using Signac) were retained for downstream analysis: percent mitochondrial RNA reads < 10%; $3 > \log_{10}$(ATAC counts) < 4.5; $3 > \log_{10}$(RNA/UMI counts) < 4.5; Fraction of reads in peaks > 40%; TSS percentile > 75%. RNA/UMI counts were subject to a variance-stabilized normalization procedure using Seurat's (76) 'glmGamPoi' (77) function prior to dimensionality reduction using PCA. ATAC data after TFIDF/SVD (75) dimensionality reduction was integrated with reduced-dimensionality RNA data (PCA matrix) using the WNN (78) function with default parameters. CD4 and CD8 cells were defined using absolute RNA/UMI counts greater than 0. Cells with counts for both CD4 and CD8 were further excluded. Clusters were identified using the standard Seurat workflow. Gene activity scores and Motif scores were calculated using Signac (75) and ChromVar (79).

External Data

To identify genes specific for Tscm cells, publicly available data single cell RNA sequencing data were obtained from GEO (GSE152379) and processed using Seurat. To generate a high confidence list of Tscm-specific genes, we identified those genes specific to BACH2 overexpressing cells (9) using a strict filter of a q value of < 0.001 and $\log_2$ fold change of > 1, removing ribosomal protein genes (Rpl* and Rps*) and included critical Tscm genes, Bach2, Bcl2, Eomes, Myb, Tnfsf8. Gene set for exhaustion (Tex) was generated taking data from published bulk expression profiles (29) and filtered using the same cutoffs. Gene set

scores were calculated using the AddModuleScore function in Seurat. Statistical test for gene set scores was calculated using Wilcoxon rank sum in R.

Human Samples

PBMC from an IRB approved study of immune reconstitution in patients receiving allogeneic stem cell transplantation at the Fred Hutchinson Cancer Center were thawed and resuspended in pre-warmed culture media containing DNase1. Cells were washed twice with PBS prior to incubating with FVS440UV (BD Biosciences) and Fc Block (Human TruStain, Biolegend) for 15 minutes at room temperature. Cells were washed and then stained with surface flow cytometry antibodies for 30 minutes on ice. Cells were washed and fixed with eBioscience FoxP3 staining kit according to manufacturer's protocol prior to intracellular staining at room temperature for 1 hour.

Statistical analysis—Data presented as mean ± SEM and $p<0.05$ was considered significant. Survival curves were plotted using Kaplan-Meier estimates and compared by Log-rank (Mantel-Cox) test. M-bands were modeled as previously described (3, 19) and the M-band relapse threshold (G/A above 0.282) has been previously reported (3, 19). Competing risk analysis was performed using the cmprsk R package. Comparisons between two groups were performed with t-test or Mann-Whitney *U* test and comparisons between three or more groups were performed with one-way ANOVA and Tukey's multiple comparisons test for normally distributed data or with Kruskal-Wallis and Dunn's multiple comparisons test for nonparametric data.

Supplementary Material

Refer to Web version on PubMed Central for supplementary material.

Acknowledgements:

We thank the Fred Hutch Vaccine and Infectious Disease Division for the support of the peripheral blood mononuclear cell biorepository.

Funding:

SAM is funded by a Klorfine fellowship and ASTCT New Investigator Award. DZ is funded by a K23 award (1K23AI163343–01A1). This work was supported by an NIH/NCI P01 award (CA078902).

SM, GRH and AMR have filed a provisional patent application on the use of DR-18 in hematological malignancies. GRH has consulted for Generon Corporation, NapaJen Pharma, iTeos Therapeutics, Neoleukin Therapeutics and has received research funding from Compass Therapeutics, Syndax Pharmaceuticals, Applied Molecular Transport, Serplus Technology, Heat Biologics, Laevoroc Oncology and iTeos Therapeutics. KAM is on the scientific advisory board for Postbiotics Plus. SWL is on the advisory board for Janssen, Astellas, Celgene/BMS and Novartis and has received research funding from Janssen, Celgene/BMS and a speaker's honorarium from AbbVie. AMR is on the board of directors, has consulted for, has ownership interest and intellectual property in, and has received research funding from Simcha Therapeutics, the commercial licensee of the DR-18 program. AS is on the advisory board for BMS, Janssen, Secura Bio, AbbVie, Haemalogix, Pfizer, Roche, Amgen, and Antegene. AS received speaker's bureau from BMS and Janssen, research support from BMS, Janssen, Amgen, Haemalogix, AbbVie, PharmaMar, and honoraria from BMS, Janssen, Amgen, Secura Bio, AbbVie, Haemalogix, Pfizer, Roche, Antegene.

Data and materials availability

New RNA sequencing data are available at the Gene Expression Omnibus (GEO) repository under accession number GSE211464. DR-18 was provided by Simcha Therapeutics under an MTA and requests for access should be addressed to Dr. Aaron Ring (aaron.ring@yale.edu). All other data needed to evaluate the conclusions in the paper are present in the paper or the Supplementary Materials.

References and notes

1. Blank CU, Haining WN, Held W, Hogan PG, Kallies A, Lugli E, Lynn RC, Philip M, Rao A, Restifo NP, Schietinger A, Schumacher TN, Schwartzberg PL, Sharpe AH, Speiser DE, Wherry EJ, Youngblood BA, Zehn D, Defining 'T cell exhaustion'. Nature Reviews Immunology, (2019).
2. Chung DJ, Pronschinske KB, Shyer JA, Sharma S, Leung S, Curran SA, Lesokhin AM, Devlin SM, Giralt SA, Young JW, T-cell Exhaustion in Multiple Myeloma Relapse after Autotransplant: Optimal Timing of Immunotherapy. Cancer Immunol Res 4, 61–71 (2016). [PubMed: 26464015]
3. Minnie SA, Kuns RD, Gartlan KH, Zhang P, Wilkinson AN, Samson L, Guillerey C, Engwerda C, MacDonald KPA, Smyth MJ, Markey KA, Vuckovic S, Hill GR, Myeloma escape after stem cell transplantation is a consequence of T-cell exhaustion and is prevented by TIGIT blockade. Blood 132, 1675–1688 (2018). [PubMed: 30154111]
4. Zelle-Rieser C, Thangavadivel S, Biedermann R, Brunner A, Stoitzner P, Willenbacher E, Greil R, Johrer K, T cells in multiple myeloma display features of exhaustion and senescence at the tumor site. J Hematol Oncol 9, 116 (2016). [PubMed: 27809856]
5. Haslam A, Prasad V, Estimation of the Percentage of US Patients With Cancer Who Are Eligible for and Respond to Checkpoint Inhibitor Immunotherapy Drugs. JAMA network open 2, e192535 (2019).
6. Armand P, Engert A, Younes A, Fanale M, Santoro A, Zinzani PL, Timmerman JM, Collins GP, Ramchandren R, Cohen JB, De Boer JP, Kuruvilla J, Savage KJ, Trneny M, Shipp MA, Kato K, Sumbul A, Farsaci B, Ansell SM, Nivolumab for Relapsed/Refractory Classic Hodgkin Lymphoma After Failure of Autologous Hematopoietic Cell Transplantation: Extended Follow-Up of the Multicohort Single-Arm Phase II CheckMate 205 Trial. Journal of clinical oncology : official journal of the American Society of Clinical Oncology 36, 1428–1439 (2018). [PubMed: 29584546]
7. Ramchandren R, Domingo-Domènech E, Rueda A, Trněný M, Feldman TA, Lee HJ, Provencio M, Sillaber C, Cohen JB, Savage KJ, Willenbacher W, Ligon AH, Ouyang J, Redd R, Rodig SJ, Shipp MA, Sacchi M, Sumbul A, Armand P, Ansell SM, Nivolumab for Newly Diagnosed Advanced-Stage Classic Hodgkin Lymphoma: Safety and Efficacy in the Phase II CheckMate 205 Study. Journal of clinical oncology : official journal of the American Society of Clinical Oncology 37, 1997–2007 (2019). [PubMed: 31112476]
8. Siddiqui I, Schaeuble K, Chennupati V, Fuertes Marraco SA, Calderon-Copete S, Pais Ferreira D, Carmona SJ, Scarpellino L, Gfeller D, Pradervand S, Luther SA, Speiser DE, Held W, Intratumoral Tcf1+PD-1+CD8+ T Cells with Stem-like Properties Promote Tumor Control in Response to Vaccination and Checkpoint Blockade Immunotherapy. Immunity 50, 195–211.e110 (2019).
9. Yao C, Lou G, Sun HW, Zhu Z, Sun Y, Chen Z, Chauss D, Moseman EA, Cheng J, D'Antonio MA, Shi W, Shi J, Kometani K, Kurosaki T, Wherry EJ, Afzali B, Gattinoni L, Zhu Y, McGavern DB, O'Shea JJ, Schwartzberg PL, Wu T, BACH2 enforces the transcriptional and epigenetic programs of stem-like CD8(+) T cells. Nature immunology 22, 370–380 (2021). [PubMed: 33574619]
10. Fraietta JA, Lacey SF, Orlando EJ, Pruteanu-Malinici I, Gohil M, Lundh S, Boesteanu AC, Wang Y, O'Connor RS, Hwang WT, Pequignot E, Ambrose DE, Zhang C, Wilcox N, Bedoya F, Dorfmeier C, Chen F, Tian L, Parakandi H, Gupta M, Young RM, Johnson FB, Kulikovskaya I, Liu L, Xu J, Kassim SH, Davis MM, Levine BL, Frey NV, Siegel DL, Huang AC, Wherry EJ, Bitter H, Brogdon JL, Porter DL, June CH, Melenhorst JJ, Determinants of response and resistance to CD19 chimeric antigen receptor (CAR) T cell therapy of chronic lymphocytic leukemia. Nat Med 24, 563–571 (2018). [PubMed: 29713085]

11. Aschan J, Lonnqvist B, Ringden O, Kumlien G, Gahrton G, Graft-versus-myeloma effect. Lancet 348, 346 (1996).
12. Tricot G, Vesole DH, Jagannath S, Hilton J, Munshi N, Barlogie B, Graft-versus-myeloma effect: proof of principle. Blood 87, 1196–1198 (1996). [PubMed: 8562947]
13. Bensinger WI, Role of autologous and allogeneic stem cell transplantation in myeloma. Leukemia 23, 442–448 (2009). [PubMed: 19277049]
14. Ijaz A, Khan AY, Malik SU, Faridi W, Fraz MA, Usman M, Tariq MJ, Durer S, Durer C, Russ A, Parr NNC, Baig Z, Sagar FNU, Ali Z, McBride A, Anwer F, Significant Risk of Graft-versus-Host Disease with Exposure to Checkpoint Inhibitors before and after Allogeneic Transplantation. Biology of Blood and Marrow Transplantation 25, 94–99 (2019). [PubMed: 30195074]
15. Haverkos BM, Abbott D, Hamadani M, Armand P, Flowers ME, Merryman R, Kamdar M, Kanate AS, Saad A, Mehta A, Ganguly S, Fenske TS, Hari P, Lowsky R, Andritsos L, Jagasia M, Bashey A, Brown S, Bachanova V, Stephens D, Mineishi S, Nakamura R, Chen Y-B, Blazar BR, Gutman J, Devine SM, PD-1 blockade for relapsed lymphoma post–allogeneic hematopoietic cell transplant: high response rate but frequent GVHD. Blood 130, 221–228 (2017). [PubMed: 28468799]
16. Rovatti PE, Gambacorta V, Lorentino F, Ciceri F, Vago L, Mechanisms of Leukemia Immune Evasion and Their Role in Relapse After Haploidentical Hematopoietic Cell Transplantation. Front Immunol 11, 147–147 (2020). [PubMed: 32158444]
17. Yin X, Tang L, Fan F, Jiang Q, Sun C, Hu Y, Allogeneic stem-cell transplantation for multiple myeloma: a systematic review and meta-analysis from 2007 to 2017. Cancer cell international 18, 62–62 (2018). [PubMed: 29713245]
18. Stern M, de Wreede LC, Brand R, van Biezen A, Dreger P, Mohty M, de Witte TM, Kröger N, Ruutu T, Sensitivity of hematological malignancies to graft-versus-host effects: an EBMT megafile analysis. Leukemia 28, 2235–2240 (2014). [PubMed: 24781016]
19. Vuckovic S, Minnie SA, Smith D, Gartlan KH, Watkins TS, Markey KA, Mukhopadhyay P, Guillerey C, Kuns RD, Locke KR, Pritchard AL, Johansson PA, Varelias A, Zhang P, Huntington ND, Waddell N, Chesi M, Miles JJ, Smyth MJ, Hill GR, Bone marrow transplantation generates T cell-dependent control of myeloma in mice. J Clin Invest 129, 106–121 (2019). [PubMed: 30300141]
20. Inozume T, Hanada K, Wang QJ, Ahmadzadeh M, Wunderlich JR, Rosenberg SA, Yang JC, Selection of CD8+PD-1+ lymphocytes in fresh human melanomas enriches for tumor-reactive T cells. Journal of immunotherapy (Hagerstown, Md. : 1997) 33, 956–964 (2010). [PubMed: 20948441]
21. Braun M, Aguilera AR, Sundarrajan A, Corvino D, Stannard K, Krumeich S, Das I, Lima LG, Meza Guzman LG, Li K, Li R, Salim N, Jorge MV, Ham S, Kelly G, Vari F, Lepletier A, Raghavendra A, Pearson S, Madore J, Jacquelin S, Effern M, Quine B, Koufariotis LT, Casey M, Nakamura K, Seo EY, Hölzel M, Geyer M, Kristiansen G, Taheri T, Ahern E, Hughes BGM, Wilmott JS, Long GV, Scolyer RA, Batstone MD, Landsberg J, Dietrich D, Pop OT, Flatz L, Dougall WC, Veillette A, Nicholson SE, Möller A, Johnston RJ, Martinet L, Smyth MJ, Bald T, CD155 on Tumor Cells Drives Resistance to Immunotherapy by Inducing the Degradation of the Activating Receptor CD226 in CD8(+) T Cells. Immunity 53, 805–823.e815 (2020).
22. Yu X, Harden K, Gonzalez LC, Francesco M, Chiang E, Irving B, Tom I, Ivelja S, Refino CJ, Clark H, Eaton D, Grogan JL, The surface protein TIGIT suppresses T cell activation by promoting the generation of mature immunoregulatory dendritic cells. Nature immunology 10, 48–57 (2009). [PubMed: 19011627]
23. Herbaux C, Gauthier J, Brice P, Drumez E, Ysebaert L, Doyen H, Fornecker L, Bouabdallah K, Manson G, Ghesquières H, Tabrizi R, Hermet E, Lazarovici J, Thiebaut-Bertrand A, Chauchet A, Demarquette H, Boyle E, Houot R, Yakoub-Agha I, Morschhauser F, Efficacy and tolerability of nivolumab after allogeneic transplantation for relapsed Hodgkin lymphoma. Blood 129, 2471–2478 (2017). [PubMed: 28270452]
24. Blazar BR, Carreno BM, Panoskaltsis-Mortari A, Carter L, Iwai Y, Yagita H, Nishimura H, Taylor PA, Blockade of Programmed Death-1 Engagement Accelerates Graft-Versus-Host Disease Lethality by an IFN-γ-Dependent Mechanism. The Journal of Immunology 171, 1272–1277 (2003). [PubMed: 12874215]

25. Saha A, Aoyama K, Taylor PA, Koehn BH, Veenstra RG, Panoskaltsis-Mortari A, Munn DH, Murphy WJ, Azuma M, Yagita H, Fife BT, Sayegh MH, Najafian N, Socie G, Ahmed R, Freeman GJ, Sharpe AH, Blazar BR, Host programmed death ligand 1 is dominant over programmed death ligand 2 expression in regulating graft-versus-host disease lethality. Blood 122, 3062–3073 (2013). [PubMed: 24030385]
26. Wu L, Mao L, Liu J-F, Chen L, Yu G-T, Yang L-L, Wu H, Bu L-L, Kulkarni AB, Zhang W-F, Sun Z-J, Blockade of TIGIT/CD155 Signaling Reverses T-cell Exhaustion and Enhances Antitumor Capability in Head and Neck Squamous Cell Carcinoma. Cancer Immunology Research 7, 1700 (2019). [PubMed: 31387897]
27. Preillon J, Cuende J, Rabolli V, Garnero L, Mercier M, Wald N, Pappalardo A, Denies S, Jamart D, Michaux AC, Pirson R, Pitard V, Bagot M, Prasad S, Houthuys E, Brouwer M, Marillier R, Lambolez F, Marchante JR, Nyawouame F, Carter MJ, Baron-Bodo V, Marie-Cardine A, Cragg M, Déchanet-Merville J, Driessens G, Hoofd C, Restoration of T-cell Effector Function, Depletion of Tregs, and Direct Killing of Tumor Cells: The Multiple Mechanisms of Action of a-TIGIT Antagonist Antibodies. Mol Cancer Ther 20, 121–131 (2021). [PubMed: 33277440]
28. Philip M, Fairchild L, Sun L, Horste EL, Camara S, Shakiba M, Scott AC, Viale A, Lauer P, Merghoub T, Hellmann MD, Wolchok JD, Leslie CS, Schietinger A, Chromatin states define tumour-specific T cell dysfunction and reprogramming. Nature 545, 452–456 (2017). [PubMed: 28514453]
29. Scott AC, Dundar F, Zumbo P, Chandran SS, Klebanoff CA, Shakiba M, Trivedi P, Menocal L, Appleby H, Camara S, Zamarin D, Walther T, Snyder A, Femia MR, Comen EA, Wen HY, Hellmann MD, Anandasabapathy N, Liu Y, Altorki NK, Lauer P, Levy O, Glickman MS, Kaye J, Betel D, Philip M, Schietinger A, TOX is a critical regulator of tumour-specific T cell differentiation. Nature 571, 270–274 (2019). [PubMed: 31207604]
30. Liu X, Wang Y, Lu H, Li J, Yan X, Xiao M, Hao J, Alekseev A, Khong H, Chen T, Huang R, Wu J, Zhao Q, Wu Q, Xu S, Wang X, Jin W, Yu S, Wang Y, Wei L, Wang A, Zhong B, Ni L, Liu X, Nurieva R, Ye L, Tian Q, Bian XW, Dong C, Genome-wide analysis identifies NR4A1 as a key mediator of T cell dysfunction. Nature 567, 525–529 (2019). [PubMed: 30814730]
31. Martinez GJ, Pereira RM, Äijö T, Kim EY, Marangoni F, Pipkin ME, Togher S, Heissmeyer V, Zhang YC, Crotty S, Lamperti ED, Ansel KM, Mempel TR, Lähdesmäki H, Hogan PG, Rao A, The transcription factor NFAT promotes exhaustion of activated $CD8^+$ T cells. Immunity 42, 265–278 (2015). [PubMed: 25680272]
32. Pais Ferreira D, Silva JG, Wyss T, Fuertes Marraco SA, Scarpellino L, Charmoy M, Maas R, Siddiqui I, Tang L, Joyce JA, Delorenzi M, Luther SA, Speiser DE, Held W, Central memory CD8+ T cells derive from stem-like Tcf7hi effector cells in the absence of cytotoxic differentiation. Immunity 53, 985–1000.e1011 (2020).
33. Hudson WH, Gensheimer J, Hashimoto M, Wieland A, Valanparambil RM, Li P, Lin J-X, Konieczny BT, Im SJ, Freeman GJ, Leonard WJ, Kissick HT, Ahmed R, Proliferating Transitory T Cells with an Effector-like Transcriptional Signature Emerge from PD-1+ Stem-like CD8+ T Cells during Chronic Infection. Immunity 51, 1043–1058.e1044 (2019).
34. Huang AC, Postow MA, Orlowski RJ, Mick R, Bengsch B, Manne S, Xu W, Harmon S, Giles JR, Wenz B, Adamow M, Kuk D, Panageas KS, Carrera C, Wong P, Quagliarello F, Wubbenhorst B, D'Andrea K, Pauken KE, Herati RS, Staupe RP, Schenkel JM, McGettigan S, Kothari S, George SM, Vonderheide RH, Amaravadi RK, Karakousis GC, Schuchter LM, Xu X, Nathanson KL, Wolchok JD, Gangadhar TC, Wherry EJ, T-cell invigoration to tumour burden ratio associated with anti-PD-1 response. Nature 545, 60–65 (2017). [PubMed: 28397821]
35. Zhou T, Damsky W, Weizman O-E, McGeary MK, Hartmann KP, Rosen CE, Fischer S, Jackson R, Flavell RA, Wang J, Sanmamed MF, Bosenberg MW, Ring AM, IL-18BP is a secreted immune checkpoint and barrier to IL-18 immunotherapy. Nature 583, 609–614 (2020). [PubMed: 32581358]
36. Clénet M-L, Gagnon F, Moratalla AC, Viel EC, Arbour N, Peripheral human CD4(+)CD8(+) T lymphocytes exhibit a memory phenotype and enhanced responses to IL-2, IL-7 and IL-15. Sci Rep 7, 11612–11612 (2017).
37. Guillerey C, Nakamura K, Pichler AC, Barkauskas D, Krumeich S, Stannard K, Miles K, Harjunpaa H, Yu Y, Casey M, Doban AI, Lazar M, Hartel G, Smith D, Vuckovic S, Teng MW,

Bergsagel PL, Chesi M, Hill GR, Martinet L, Smyth MJ, Chemotherapy followed by anti-CD137 mAb immunotherapy improves disease control in a mouse myeloma model. JCI Insight 5, (2019).

38. Van Gassen S, Callebaut B, Van Helden MJ, Lambrecht BN, Demeester P, Dhaene T, Saeys Y, FlowSOM: Using self-organizing maps for visualization and interpretation of cytometry data. Cytometry. Part A : the journal of the International Society for Analytical Cytology 87, 636–645 (2015). [PubMed: 25573116]
39. Cretney E, Xin A, Shi W, Minnich M, Masson F, Miasari M, Belz GT, Smyth GK, Busslinger M, Nutt SL, Kallies A, The transcription factors Blimp-1 and IRF4 jointly control the differentiation and function of effector regulatory T cells. Nature immunology 12, 304–311 (2011). [PubMed: 21378976]
40. Zhou M, Sacirbegovic F, Zhao K, Rosenberger S, Shlomchik WD, T cell exhaustion and a failure in antigen presentation drive resistance to the graft-versus-leukemia effect. Nature Communications 11, 4227 (2020).
41. Fionda C, Abruzzese MP, Zingoni A, Cecere F, Vulpis E, Peruzzi G, Soriani A, Molfetta R, Paolini R, Ricciardi MR, Petrucci MT, Santoni A, Cippitelli M, The IMiDs targets IKZF-1/3 and IRF4 as novel negative regulators of NK cell-activating ligands expression in multiple myeloma. Oncotarget 6, 23609–23630 (2015).
42. El-Sherbiny YM, Meade JL, Holmes TD, McGonagle D, Mackie SL, Morgan AW, Cook G, Feyler S, Richards SJ, Davies FE, Morgan GJ, Cook GP, The Requirement for DNAM-1, NKG2D, and NKp46 in the Natural Killer Cell-Mediated Killing of Myeloma Cells. Cancer Research 67, 8444–8449 (2007). [PubMed: 17875681]
43. Yousef S, Marvin J, Steinbach M, Langemo A, Kovacsovics T, Binder M, Kroger N, Luetkens T, Atanackovic D, Immunomodulatory molecule PD-L1 is expressed on malignant plasma cells and myeloma-propagating pre-plasma cells in the bone marrow of multiple myeloma patients. Blood cancer journal 5, e285 (2015).
44. Bahlis NJ, King AM, Kolonias D, Carlson LM, Liu HY, Hussein MA, Terebelo HR, Byrne GE Jr., Levine BL, Boise LH, Lee KP, CD28-mediated regulation of multiple myeloma cell proliferation and survival. Blood 109, 5002–5010 (2007). [PubMed: 17311991]
45. Ishibashi M, Tamura H, Sunakawa M, Kondo-Onodera A, Okuyama N, Hamada Y, Moriya K, Choi I, Tamada K, Inokuchi K, Myeloma Drug Resistance Induced by Binding of Myeloma B7-H1 (PD-L1) to PD-1. Cancer Immunology Research 4, 779–788 (2016). [PubMed: 27440711]
46. Wang L, Wang H, Chen H, Wang WD, Chen XQ, Geng QR, Xia ZJ, Lu Y, Serum levels of soluble programmed death ligand 1 predict treatment response and progression free survival in multiple myeloma. Oncotarget 6, 41228–41236 (2015). [PubMed: 26515600]
47. Roemer MGM, Redd RA, Cader FZ, Pak CJ, Abdelrahman S, Ouyang J, Sasse S, Younes A, Fanale M, Santoro A, Zinzani PL, Timmerman J, Collins GP, Ramchandren R, Cohen JB, De Boer JP, Kuruvilla J, Savage KJ, Trneny M, Ansell S, Kato K, Farsaci B, Sumbul A, Armand P, Neuberg DS, Pinkus GS, Ligon AH, Rodig SJ, Shipp MA, Major Histocompatibility Complex Class II and Programmed Death Ligand 1 Expression Predict Outcome After Programmed Death 1 Blockade in Classic Hodgkin Lymphoma. Journal of clinical oncology : official journal of the American Society of Clinical Oncology 36, 942–950 (2018). [PubMed: 29394125]
48. Prestipino A, Emhardt AJ, Aumann K, O'Sullivan D, Gorantla SP, Duquesne S, Melchinger W, Braun L, Vuckovic S, Boerries M, Busch H, Halbach S, Pennisi S, Poggio T, Apostolova P, Veratti P, Hettich M, Niedermann G, Bartholomä M, Shoumariyeh K, Jutzi JS, Wehrle J, Dierks C, Becker H, Schmitt-Graeff A, Follo M, Pfeifer D, Rohr J, Fuchs S, Ehl S, Hartl FA, Minguet S, Miething C, Heidel FH, Kröger N, Triviai I, Brummer T, Finke J, Illert AL, Ruggiero E, Bonini C, Duyster J, Pahl HL, Lane SW, Hill GR, Blazar BR, von Bubnoff N, Pearce EL, Zeiser R, Oncogenic JAK2(V617F) causes PD-L1 expression, mediating immune escape in myeloproliferative neoplasms. Sci Transl Med 10, (2018).
49. Norde WJ, Maas F, Hobo W, Korman A, Quigley M, Kester MG, Hebeda K, Falkenburg JH, Schaap N, de Witte TM, van der Voort R, Dolstra H, PD-1/PD-L1 interactions contribute to functional T-cell impairment in patients who relapse with cancer after allogeneic stem cell transplantation. Cancer Res 71, 5111–5122 (2011). [PubMed: 21659460]

50. Joller N, Hafler JP, Brynedal B, Kassam N, Spoerl S, Levin SD, Sharpe AH, Kuchroo VK, Cutting edge: TIGIT has T cell-intrinsic inhibitory functions. Journal of immunology (Baltimore, Md. : 1950) 186, 1338–1342 (2011). [PubMed: 21199897]
51. Rosenblatt J, Avigan D, Targeting the PD-1/PD-L1 axis in multiple myeloma: a dream or a reality? Blood 129, 275–279 (2017). [PubMed: 27919908]
52. Noviello M, Manfredi F, Ruggiero E, Perini T, Oliveira G, Cortesi F, De Simone P, Toffalori C, Gambacorta V, Greco R, Peccatori J, Casucci M, Casorati G, Dellabona P, Onozawa M, Teshima T, Griffioen M, Halkes CJM, Falkenburg JHF, Stölzel F, Altmann H, Bornhäuser M, Waterhouse M, Zeiser R, Finke J, Cieri N, Bondanza A, Vago L, Ciceri F, Bonini C, Bone marrow central memory and memory stem T-cell exhaustion in AML patients relapsing after HSCT. Nature Communications 10, 1065 (2019).
53. Simonetta F, Pradier A, Bosshard C, Masouridi-Levrat S, Dantin C, Koutsi A, Tirefort Y, Roosnek E, Chalandon Y, Dynamics of Expression of Programmed Cell Death Protein-1 (PD-1) on T Cells After Allogeneic Hematopoietic Stem Cell Transplantation. Front Immunol 10, 1034 (2019). [PubMed: 31156625]
54. Hutten TJA, Norde WJ, Woestenenk R, Wang RC, Maas F, Kester M, Falkenburg JHF, Berglund S, Luznik L, Jansen JH, Schaap N, Dolstra H, Hobo W, Increased Coexpression of PD-1, TIGIT, and KLRG-1 on Tumor-Reactive CD8+ T Cells During Relapse after Allogeneic Stem Cell Transplantation. Biology of Blood and Marrow Transplantation 24, 666–677 (2018). [PubMed: 29197680]
55. Roberto A, Castagna L, Zanon V, Bramanti S, Crocchiolo R, McLaren JE, Gandolfi S, Tentorio P, Sarina B, Timofeeva I, Santoro A, Carlo-Stella C, Bruno B, Carniti C, Corradini P, Gostick E, Ladell K, Price DA, Roederer M, Mavilio D, Lugli E, Role of naive-derived T memory stem cells in T-cell reconstitution following allogeneic transplantation. Blood 125, 2855–2864 (2015). [PubMed: 25742699]
56. Cieri N, Camisa B, Cocchiarella F, Forcato M, Oliveira G, Provasi E, Bondanza A, Bordignon C, Peccatori J, Ciceri F, Lupo-Stanghellini MT, Mavilio F, Mondino A, Bicciato S, Recchia A, Bonini C, IL-7 and IL-15 instruct the generation of human memory stem T cells from naive precursors. Blood 121, 573–584 (2013). [PubMed: 23160470]
57. Yang Y-G, Qi J, Wang M-G, Sykes M, Donor-derived interferon γ separates graft-versus-leukemia effects and graft-versus-host disease induced by donor CD8 T cells. Blood 99, 4207–4215 (2002). [PubMed: 12010827]
58. Wachsmuth LP, Patterson MT, Eckhaus MA, Venzon DJ, Gress RE, Kanakry CG, Posttransplantation cyclophosphamide prevents graft-versus-host disease by inducing alloreactive T cell dysfunction and suppression. The Journal of Clinical Investigation 129, 2357–2373 (2019). [PubMed: 30913039]
59. Wachsmuth LP, Patterson MT, Eckhaus MA, Venzon DJ, Kanakry CG, Optimized Timing of Post-Transplantation Cyclophosphamide in MHC-Haploidentical Murine Hematopoietic Cell Transplantation. Biol Blood Marrow Transplant 26, 230–241 (2020). [PubMed: 31586477]
60. Brissot E, Labopin M, Ehninger G, Stelljes M, Brecht A, Ganser A, Tischer J, Kröger N, Afanasyev B, Finke J, Elmaagacli A, Einsele H, Mohty M, Nagler A, Haploidentical versus unrelated allogeneic stem cell transplantation for relapsed/refractory acute myeloid leukemia: a report on 1578 patients from the Acute Leukemia Working Party of the EBMT. Haematologica 104, 524–532 (2019). [PubMed: 30361416]
61. Ciurea SO, Zhang MJ, Bacigalupo AA, Bashey A, Appelbaum FR, Aljitawi OS, Armand P, Antin JH, Chen J, Devine SM, Fowler DH, Luznik L, Nakamura R, O'Donnell PV, Perales MA, Pingali SR, Porter DL, Riches MR, Ringdén OT, Rocha V, Vij R, Weisdorf DJ, Champlin RE, Horowitz MM, Fuchs EJ, Eapen M, Haploidentical transplant with posttransplant cyclophosphamide vs matched unrelated donor transplant for acute myeloid leukemia. Blood 126, 1033–1040 (2015). [PubMed: 26130705]
62. McCurdy SR, Kasamon YL, Kanakry CG, Bolaños-Meade J, Tsai HL, Showel MM, Kanakry JA, Symons HJ, Gojo I, Smith BD, Bettinotti MP, Matsui WH, Dezern AE, Huff CA, Borrello I, Pratz KW, Gladstone DE, Swinnen LJ, Brodsky RA, Levis MJ, Ambinder RF, Fuchs EJ, Rosner GL, Jones RJ, Luznik L, Comparable composite endpoints after HLA-matched and HLA-

haploidentical transplantation with post-transplantation cyclophosphamide. Haematologica 102, 391–400 (2017). [PubMed: 27846611]

63. Rashidi A, Hamadani M, Zhang M-J, Wang H-L, Abdel-Azim H, Aljurf M, Assal A, Bajel A, Bashey A, Battiwalla M, Beitinjaneh AM, Bejanyan N, Bhatt VR, Bolaños-Meade J, Byrne M, Cahn J-Y, Cairo M, Ciurea S, Copelan E, Cutler C, Daly A, Diaz M-A, Farhadfar N, Gale RP, Ganguly S, Grunwald MR, Hahn T, Hashmi S, Hildebrandt GC, Holland HK, Hossain N, Kanakry CG, Kharfan-Dabaja MA, Khera N, Koc Y, Lazarus HM, Lee J-W, Maertens J, Martino R, McGuirk J, Munker R, Murthy HS, Nakamura R, Nathan S, Nishihori T, Palmisiano N, Patel S, Pidala J, Olin R, Olsson RF, Oran B, Ringden O, Rizzieri D, Rowe J, Savoie ML, Schultz KR, Seo S, Shaffer BC, Singh A, Solh M, Stockerl-Goldstein K, Verdonck LF, Wagner J, Waller EK, De Lima M, Sandmaier BM, Litzow M, Weisdorf D, Romee R, Saber W, Outcomes of haploidentical vs matched sibling transplantation for acute myeloid leukemia in first complete remission. Blood advances 3, 1826–1836 (2019). [PubMed: 31201170]
64. McCurdy SR, Radojcic V, Tsai HL, Vulic A, Thompson E, Ivcevic S, Kanakry CG, Powell JD, Lohman B, Adom D, Paczesny S, Cooke KR, Jones RJ, Varadhan R, Symons HJ, Luznik L, Signatures of GVHD and relapse after posttransplant cyclophosphamide revealed by immune profiling and machine learning. Blood 139, 608–623 (2022). [PubMed: 34657151]
65. Bartsch K, Al-Ali H, Reinhardt A, Franke C, Hudecek M, Kamprad M, Tschiedel S, Cross M, Niederwieser D, Gentilini C, Mesenchymal Stem Cells Remain Host-Derived Independent of the Source of the Stem-Cell Graft and Conditioning Regimen Used. Transplantation 87, (2009).
66. Ciurea SO, Schafer JR, Bassett R, Denman CJ, Cao K, Willis D, Rondon G, Chen J, Soebbing D, Kaur I, Gulbis A, Ahmed S, Rezvani K, Shpall EJ, Lee DA, Champlin RE, Phase 1 clinical trial using mbIL21 ex vivo-expanded donor-derived NK cells after haploidentical transplantation. Blood 130, 1857–1868 (2017). [PubMed: 28835441]
67. Van Elssen C, Ciurea SO, NK cell alloreactivity in acute myeloid leukemia in the post-transplant cyclophosphamide era. American journal of hematology 95, 1590–1598 (2020). [PubMed: 32857869]
68. Chesi M, Robbiani DF, Sebag M, Chng WJ, Affer M, Tiedemann R, Valdez R, Palmer SE, Haas SS, Stewart AK, Fonseca R, Kremer R, Cattoretti G, Bergsagel PL, AID-dependent activation of a MYC transgene induces multiple myeloma in a conditional mouse model of post-germinal center malignancies. Cancer cell 13, 167–180 (2008). [PubMed: 18242516]
69. Chesi M, Matthews GM, Garbitt VM, Palmer SE, Shortt J, Lefebure M, Stewart AK, Johnstone RW, Bergsagel PL, Drug response in a genetically engineered mouse model of multiple myeloma is predictive of clinical efficacy. Blood 120, 376–385 (2012). [PubMed: 22451422]
70. Markey KA, Kuns RD, Browne DJ, Gartlan KH, Robb RJ, Martins JP, Henden AS, Minnie SA, Cheong M, Koyama M, Smyth MJ, Steptoe RJ, Belz GT, Brocker T, Degli-Esposti MA, Lane SW, Hill GR, Flt-3L Expansion of Recipient CD8alpha(+) Dendritic Cells Deletes Alloreactive Donor T Cells and Represents an Alternative to Posttransplant Cyclophosphamide for the Prevention of GVHD. Clin Cancer Res 24, 1604–1616 (2018). [PubMed: 29367429]
71. Lane SW, Wang YJ, Lo Celso C, Ragu C, Bullinger L, Sykes SM, Ferraro F, Shterental S, Lin CP, Gilliland DG, Scadden DT, Armstrong SA, Williams DA, Differential niche and Wnt requirements during acute myeloid leukemia progression. Blood 118, 2849–2856 (2011). [PubMed: 21765021]
72. Markey KA, Burman AC, Banovic T, Kuns RD, Raffelt NC, Rowe V, Olver SD, Don AL, Morris ES, Pettit AR, Wilson YA, Robb RJ, Randall LM, Korner H, Engwerda CR, Clouston AD, Macdonald KP, Hill GR, Soluble lymphotoxin is an important effector molecule in GVHD and GVL. Blood 115, 122–132 (2010). [PubMed: 19789388]
73. Cooke KR, Kobzik L, Martin TR, Brewer J, Delmonte J Jr., Crawford JM, Ferrara JL, An experimental model of idiopathic pneumonia syndrome after bone marrow transplantation: I. The roles of minor H antigens and endotoxin. Blood 88, 3230–3239 (1996). [PubMed: 8963063]
74. Feng J, Liu T, Qin B, Zhang Y, Liu XS, Identifying ChIP-seq enrichment using MACS. Nat Protoc 7, 1728–1740 (2012). [PubMed: 22936215]
75. Stuart T, Srivastava A, Lareau C, Satija R, Multimodal single-cell chromatin analysis with Signac. bioRxiv, (2020).

76. Hafemeister C, Satija R, Normalization and variance stabilization of single-cell RNA-seq data using regularized negative binomial regression. Genome Biol 20, 296 (2019). [PubMed: 31870423]

77. Ahlmann-Eltze C, Huber W, glmGamPoi: fitting Gamma-Poisson generalized linear models on single cell count data. Bioinformatics 36, 5701–5702 (2021). [PubMed: 33295604]

78. Hao Y, Hao S, Andersen-Nissen E, Mauck WM 3rd, Zheng S, Butler A, Lee MJ, Wilk AJ, Darby C, Zager M, Hoffman P, Stoeckius M, Papalexi E, Mimitou EP, Jain J, Srivastava A, Stuart T, Fleming LM, Yeung B, Rogers AJ, McElrath JM, Blish CA, Gottardo R, Smibert P, Satija R, Integrated analysis of multimodal single-cell data. Cell 184, 3573–3587 e3529 (2021).

79. Schep AN, Wu B, Buenrostro JD, Greenleaf WJ, chromVAR: inferring transcription-factor-associated accessibility from single-cell epigenomic data. Nat Methods 14, 975–978 (2017). [PubMed: 28825706]

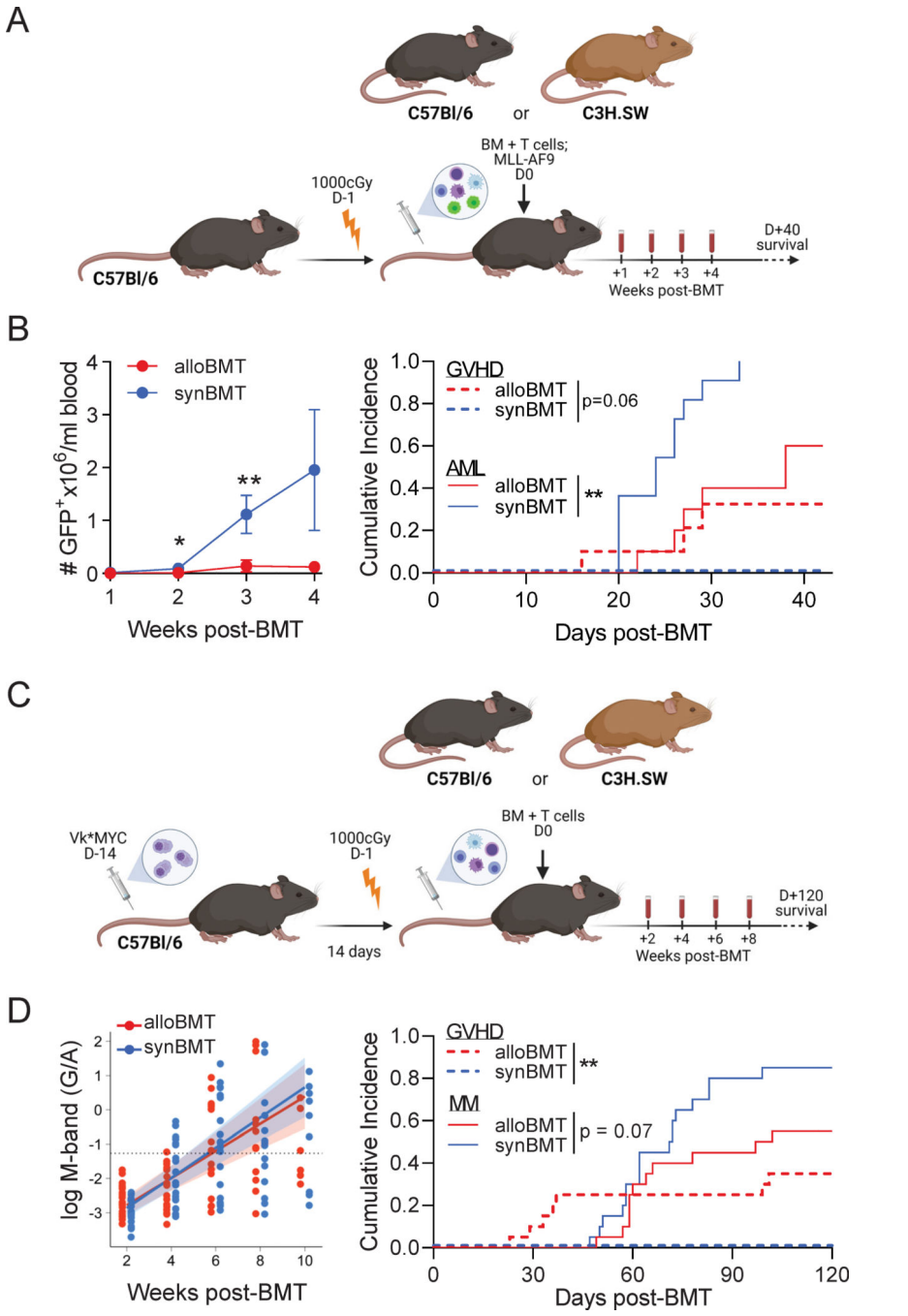

Figure 1: Graft-versus-tumor effects were subverted after alloBMT in myeloma-bearing but not leukemia-bearing recipients.

C57Bl/6 (B6) recipients injected with Vk*MYC myeloma (MM-bearing; D-14) or MLL-AF9 (AML-bearing; D0) were lethally irradiated and transplanted with 5×10^6 BM with 0.5×10^6 $CD4^+$ + 0.5×10^6 $CD8^+$ T cells from B6 (synBMT) or C3H.SW (alloBMT) donors. **(A)** Experimental schematic. **(B)** AML-bearing recipients were bled weekly to quantify the total number of circulating GFP^+ AML cells and competing risk analysis was performed to determine risk of death due to acute myeloid leukemia (AML) or GVHD. n = 11/group

from 2 experiments. Mann-Whitney *U* test for AML burden. **(C)** Experimental schematic. **(D)** MM-bearing recipients were monitored for tumor burden using M-band (G/A). M-bands were modeled to calculate a predictive rate of tumor growth (solid line), with shaded confidence intervals and M-band relapse threshold shown as dotted line. Competing risk analysis was performed to determine risk of death due to myeloma (MM) or graft-versus-host disease (GVHD). n = 20/group from 3 experiments. * $p<0.05$, ** $p<0.01$.

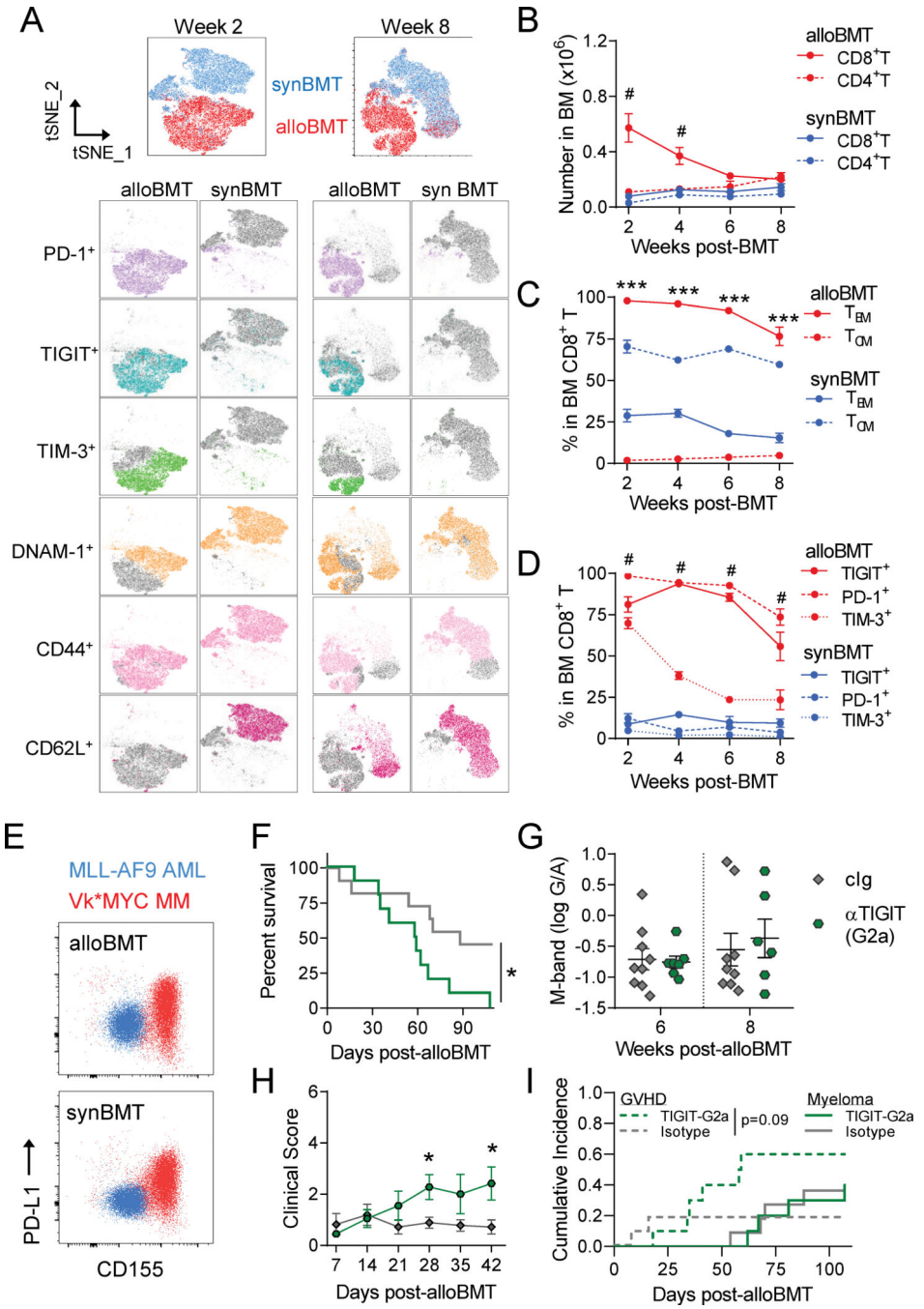

Figure 2: Alloantigen-driven inhibitory receptor expression corresponded with ligand expression on myeloma and blockade exacerbated GVHD.

B6 recipients were transplanted with 5 × 10^6 BM with 0.5 × 10^6 $CD4^+$ + 0.5 × 10^6 $CD8^+$ T cells from B6 (synBMT) or C3H.SW (alloBMT) donors. **(A-D)** BM was harvested, and T cells were phenotyped at 2, 4, 6, and 8 weeks post-transplant (n = 3–8 from 1–2 experiments). # p<0.05 when alloBMT and synBMT were compared using two-way ANOVA with Tukey's multiple comparisons test. **(A)** t-SNE analysis identified $CD8^+$ T cell clusters based on PD-1, TIGIT, TIM-3, DNAM-1, CD44 and CD62L expression at 2

weeks and 8 weeks post-transplant (n = 3–5). **(B)** $CD4^+$ and $CD8^+$ T cell number. **(C)** Frequency of effector $CD8^+$ T cells ($CD44^+CD62L^-$, T_{EM}) and central memory T cells ($CD44^+CD62L^+$, T_{CM}). **(D)** Frequency of $TIGIT^+$, $PD\text{-}1^+$, $TIM3^+$ $CD8^+$ T cells. **(E)** FACS plots of PD-L1 and CD155 expression on Vk12653 (red) and MLL-AF9 (blue). **(F- I)** Recipients were treated with 100 μg/mouse of anti-TIGIT (clone G2a; αTIGIT-G2a) or mIgG2a isotype control (cIg) twice a week from 2 weeks to 6 weeks post-transplant. **(F)** Median overall survival analyzed with Log-rank test, **(G)** M-band (log gamma/albumin) at 6 and 8 weeks after alloBMT, **(H)** clinical score and **(I)** competing risk analysis. (n = 10/group from 2 experiments). Data represent mean ± SEM. Two-way ANOVA with Tukey's multiple comparisons test. *p<0.05, ***p<0.001.

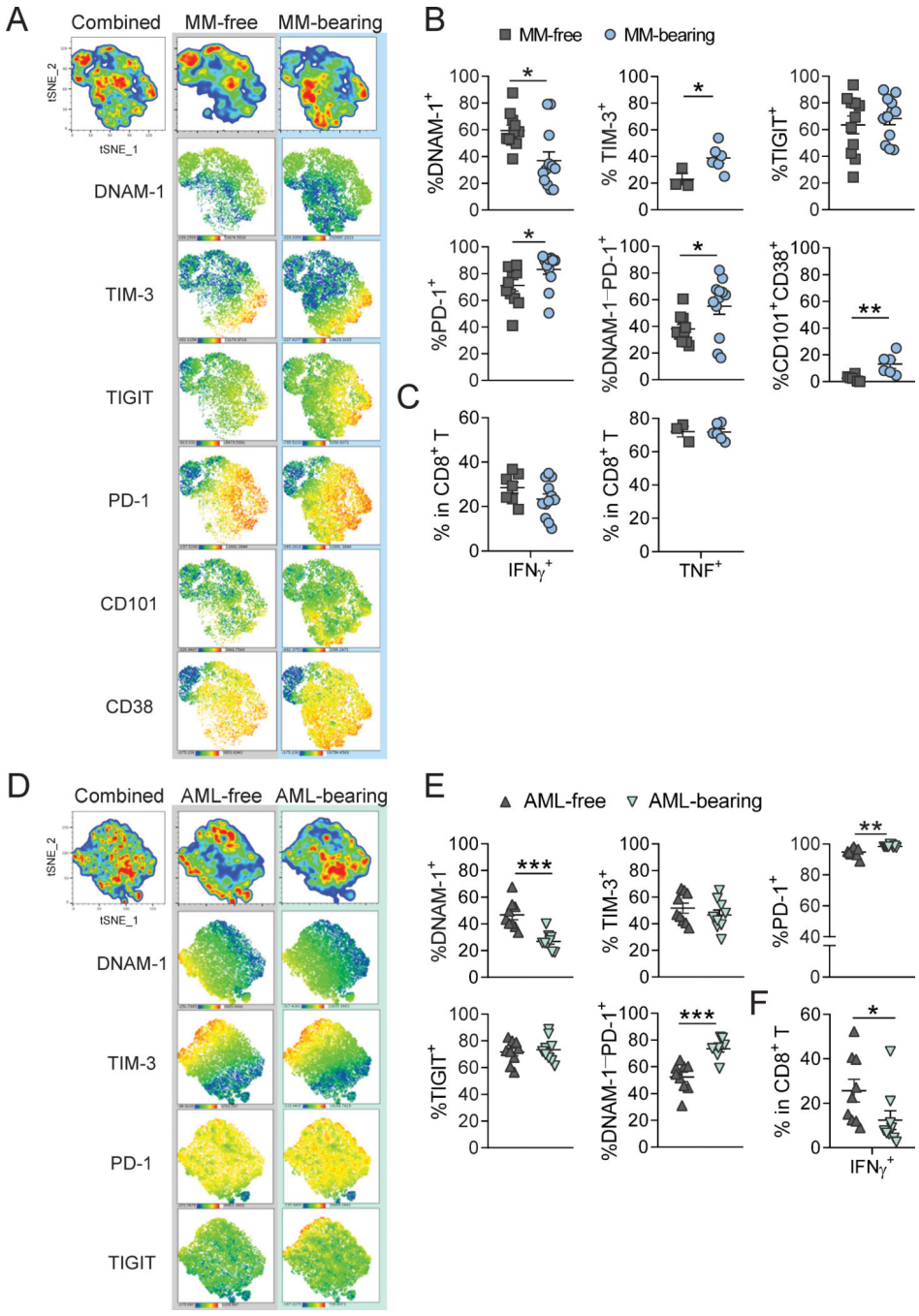

Figure 3: CD8$^+$ T cell exhaustion was primarily driven by alloantigen and not tumor antigen after alloBMT.

B6 recipients were transplanted with 5 × 10^6 BM with 0.5 × 10^6 CD4$^+$ + 0.5 × 10^6 CD8$^+$ T cells from C3H.SW (alloBMT) donors. **(A-C)** Myeloma-bearing (MM-bearing) or naïve (MM-free) recipients were sacrificed at 8 weeks post-transplant and BM was harvested to assess CD8$^+$ T cell phenotype. **(A)** representative t-SNE analysis of PD-1, TIGIT, TIM-3, DNAM-1, CD101 and CD38 expression and **(B)** frequency of DNAM-1$^+$, TIM-3$^+$, TIGIT$^+$, PD-1$^+$, DNAM-1$^-$PD-1$^+$ and CD101$^+$CD38$^+$ cells within CD8$^+$ T cells. **(C)** Frequency of

IFNγ and TNF-expressing cells within $CD8^+$ T cells after PMA/ionomycin re-stimulation. (n = 11–12/group from 2 experiments; TNF and TIM-3 n = 3–6/group from 1 experiment). **(D-F)** MLL-AF9-bearing (AML-bearing) or naïve (AML-free) mice were sacrificed 4 weeks post-transplant and BM was harvested to assess $CD8^+$ T cell phenotype. **(D)** t-SNE analysis of PD-1, TIGIT, TIM-3 and DNAM-1 expression and **(E)** frequency of DNAM-1^+, TIM-3^+, PD-1^+, $TIGIT^+$ and DNAM-1^-PD-1^+ cells within $CD8^+$ T cells. **(F)** Frequency of IFNγ-expressing cells within $CD8^+$ T cells after PMA/ionomycin re-stimulation. (n = 9/group from 2 experiments). Data represent mean ± SEM. Mann-Whitney *U* test or Student's t-test were used for numerical values. * $p<0.05$, ** $p<0.01$, *** $p<0.001$.

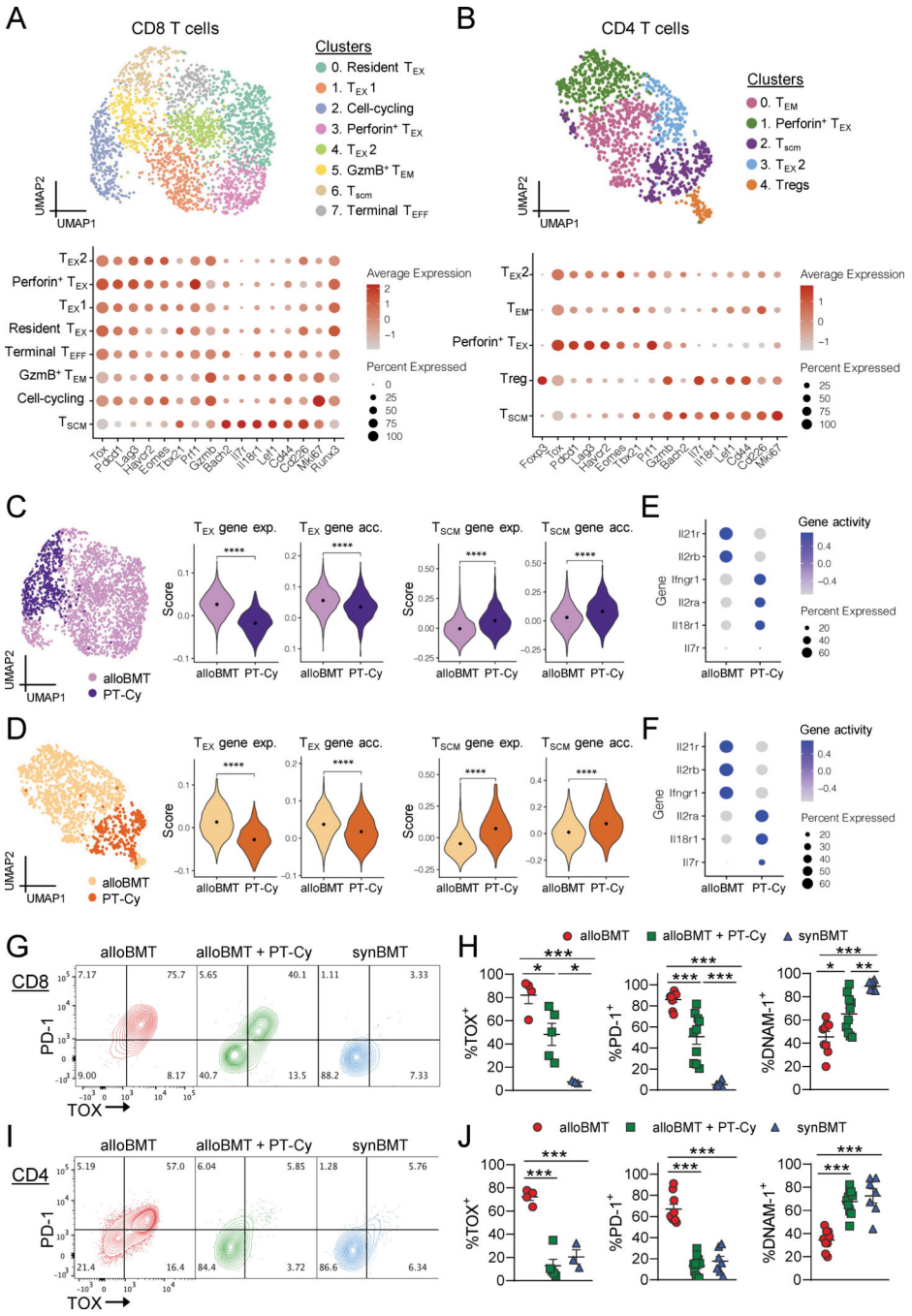

Figure 4: PT-Cy reduced alloreactive T cell exhaustion and enhanced stemness in bone marrow

B6 recipients were transplanted with 5×10^6 BM with 0.5×10^6 $CD4^+$ + 0.5×10^6 $CD8^+$ T cells from C3H.SW donors (alloBMT) or B6 donors (synBMT). Some alloBMT recipients were treated with 50 mg/kg cyclophosphamide on D+3 and D+4 after transplantation (alloBMT + PTCy). Mice were sacrificed 14 days after transplant and BM was harvested and pooled from 4 mice per group. **(A-F)** $CD8^+$ and $CD4^+$ T cells were sort purified from BM of alloBMT and alloBMT + PT-Cy recipients and nuclei were processed for 10x genomics multiome sequencing. **(A)** WNN embedding of combined ATAC and RNA data

of $CD8^+$ cells colored by cluster (top) than annotated using $CD8^+$ T cell specific markers (bottom). **(B)** $CD4^+$ T cells clustered and annotated in a manner analogous to (A). **(C)** Embedding in (A) colored by experimental group (left). Centered and scaled cumulative gene expression (abbrev. 'exp') and gene accessibility (abbrev. 'acc', using gene activity score) of T_{EX} and T_{SCM} genes in $CD8^+$ T cells by experimental group (right). Wilcoxon Rank Sum test. **(D)** Embedding in (B) colored by experimental group (left). Centered and scaled cumulative gene expression (abbrev. 'exp') and gene accessibility of T_{EX} and T_{SCM} genes in $CD4^+$ T cells by experimental group (right). Wilcoxon Rank Sum test. **(E-F)** Gene accessibility scores of key cytokine receptor genes by experiment group in **(E)** $CD8^+$ T cells and **(F)** $CD4^+$ T cells. **(G-J)** Representative flow cytometry plots of PD-1 versus TOX expression in $CD8^+$ and $CD4^+$ conventional ($FoxP3^-$) T cells. **(H)** Frequency of TOX^+, PD-1^+ and DNAM-1^+ within $CD8^+$ T cells **(J)** and $CD4^+$ conventional T cells. (n = 7–10 / group from 2 experiments, TOX n = 3 – 5 /group from 1 experiment). Data represent mean ± SEM. One-way ANOVA with Tukey's multiple comparisons test. * $p<0.05$, ** $p<0.01$, ***$p<0.001$, ****$p<0.0001$.

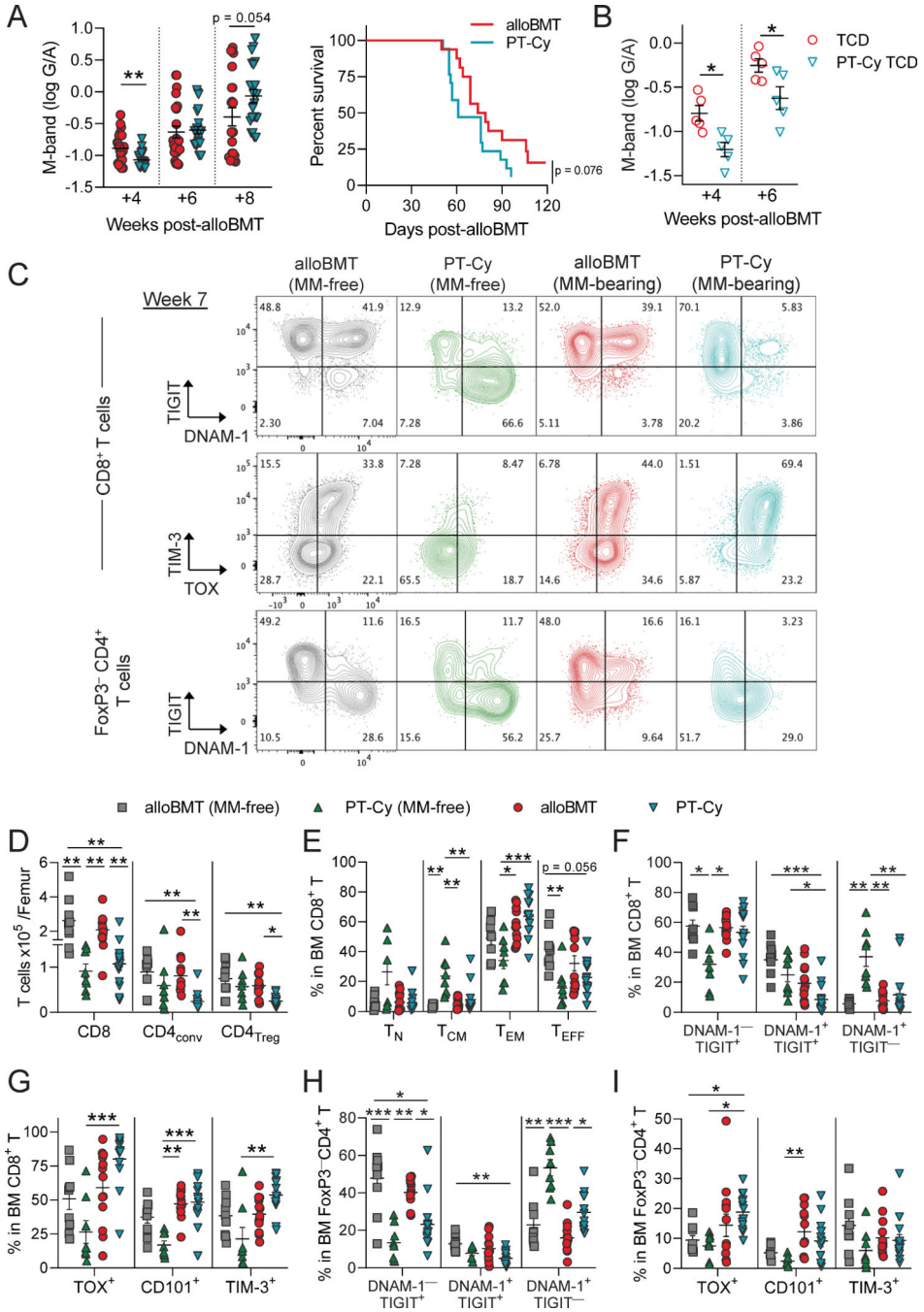

Figure 5: PT-Cy enabled the generation of myeloma-driven CD8$^+$ T cell exhaustion.

B6 MM-bearing recipients were transplanted with 5 × 10^6 BM with 0.5 × 10^6 CD8$^+$ and 0.5 × 10^6 CD4$^+$ T cells from C3H.SW donors. **(A)** MM-bearing recipients of T cell replete grafts were untreated (alloBMT) or administered 50 mg/kg cyclophosphamide on D+3 and D+4 (PT-Cy) and monitored for myeloma burden using M-band (log G/A; n = 24 from 4 experiments; Mann-Whitney *U* test) and survival (n = 17 from 3 experiments; Log-rank test). **(B)** MM-bearing recipients of T cell deplete BM grafts (TCD) were treated as above and monitored for M-band (n = 5 from 1 experiment; Student's t-test). **(C-I)** MM-bearing

and MM-naive recipients were treated as above and BM was harvested at 7 weeks post-transplant for immunophenotyping using flow cytometry (n = 8 – 14 from 2 experiments). **(C)** Representative contour plots. **(D)** $CD8^+$, conventional $CD4^+$ ($FoxP3^-$), and regulatory $CD4^+$ T cell enumeration per femur. **(E)** Frequency of naïve T (T_N; $CD44^-CD62L^-$), central memory T (T_{CM}; $CD44^+CD62L^+$), effector memory T (T_{EM}; $CD44^+CD62L^-$), and effector T (T_{EFF}; $CD44^-CD62L^-$), **(F)** DNAM-1 and TIGIT expressing cells, and **(G)** TOX^+, $CD101^+$ and $TIM\text{-}3^+$ cells within $CD8^+$ T cells. **(H)** Frequency of DNAM-1 and TIGIT expressing cells and **(I)** TOX^+, $CD101^+$ and $TIM\text{-}3^+$ cells within conventional $CD4^+$ T cells. Data represent mean ± SEM. One-way ANOVA with Tukey's multiple comparisons test or Kruskal-Wallis test with Dunn's multiple comparisons test. * $p < 0.05$ ** $p < 0.01$ *** $p < 0.001$

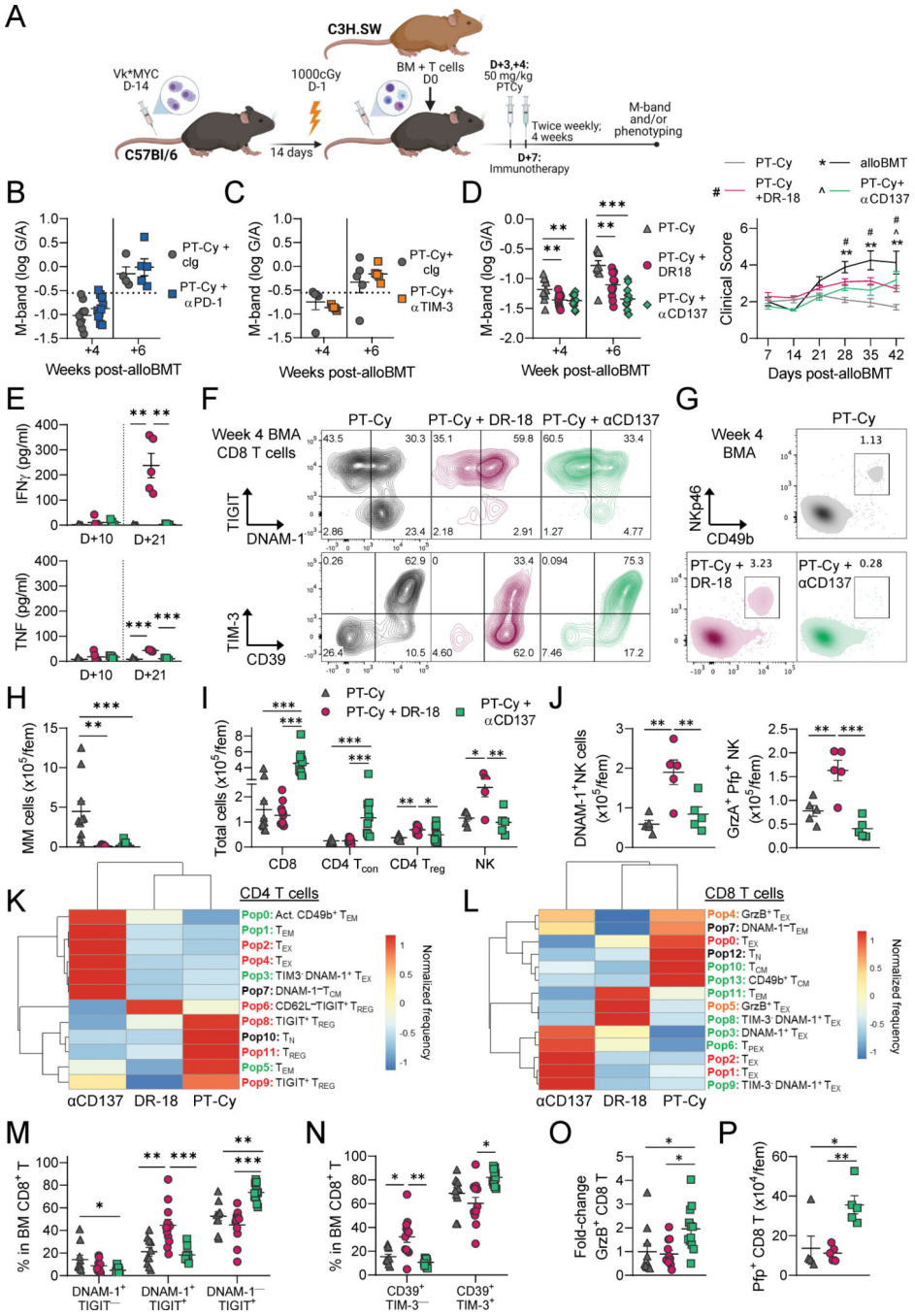

Figure 6: Agonist immunotherapy promoted GVM after PT-Cy.

B6 MM-bearing recipients were transplanted with 5×10^6 BM and 1×10^6 $CD8^+$ and 1×10^6 $CD4^+$ T cells from C3H.SW donors. Recipients were administered 50 mg/kg cyclophosphamide on D+3 and D+4 and then either a vehicle control or immunotherapy from D+7 for 4 weeks. **(A)** Experimental design. **(B)** M-band of recipients treated with rIgG2a (PT-Cy) or anti-PD-1 (PT-Cy + αPD-1). n = 10 from 2 experiments at 4 weeks; n = 5 from 1 experiment at 6 weeks. **(C)** M-band of recipients treated with rIgG2a (PT-Cy) or anti-TIM-3 (PT-Cy + αTIM-3). n = 5 from 1 experiment. **(D-P)** MM-bearing recipients

were treated with PBS (PT-Cy), or 8 μg/dose DR-18 (PT-Cy + D-18), or 100 μg/dose anti-CD137 (PT-Cy + αCD137). Bone marrow aspirates (BMA) were performed at 4 weeks post-transplant from one femur. Mice were then sacrificed at 6 weeks post-alloBMT and BM from both femurs was harvested. n = 10–12 from 2 experiments unless otherwise stated. **(D)** M-band at 4 and 6 weeks post-alloBMT and GVHD clinical (including alloBMT mice not treated with PTCy; n = 5 from 1 experiment). **(E)** IFNγ and TNF (pg/ml) in serum at D+10 and D+21 after alloBMT (n = 5 from 1 experiment). **(F)** Concatenated contour plots of TIGIT versus DNAM-1, and TIM-3 versus CD39 expression on $CD8^+$ T cells from BMA (representative of 2 experiments). **(G)** Concatenated density plots of NK cell frequency ($Nkp46^+$ $CD49b^+$) within white blood cells from BMA. **(H)** Myeloma and **(I)** T and NK cell total numbers per femur at week 6. **(J)** Number of DNAM-1^+ and granzyme A^+ perforin$^+$ ($GrzA^+Pfp^+$) NK cells (n = 5/group from 1 experiment). **(K-L)** FlowSOM clustering was performed on concatenated **(K)** $CD4^+$ and **(L)** $CD8^+$ T cells at week 6 post-transplant. Heatmaps depict relative frequencies of populations across treatment groups. Populations are colored based on expected anti-tumor properties. Green = activated effector or memory populations, orange = cytolytic, red = exhausted/suppressive and black = unknown. **(M)** Frequency of DNAM-1 and TIGIT and **(N)** CD39 and TIM-3 expressing cells within $CD8^+$ T cells at week 6. **(O)** Fold change in granzyme B ($GrzB^+$) expression on $CD8^+$ T cells and **(P)** total number of perforin-expressing (Pfp^+; n = 5/group from 1 experiment) $CD8^+$ T cells at week 6 post-transplant. Data represent mean ± SEM. One-way ANOVA with Tukey's multiple comparisons test or Kruskal-Wallis test with Dunn's multiple comparisons test. * $p < 0.05$ ** $p < 0.01$ *** $p < 0.001$.

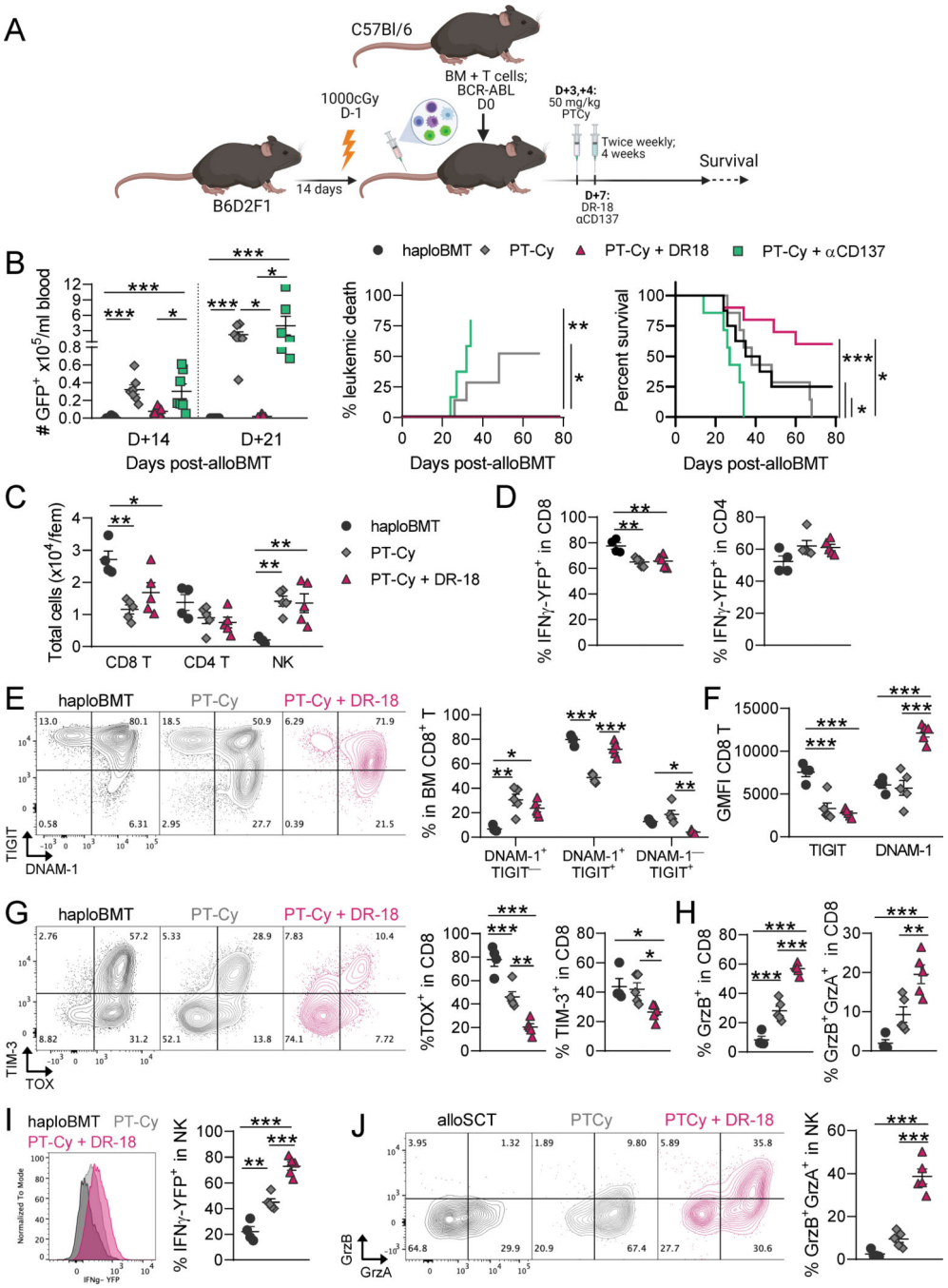

Figure 7: DR-18 promotes GVL after haploidentical transplantation.

B6D2F1 recipients were lethally irradiated and transplanted with 5 × 10^6 BM and 2 × 10^6 T cells from HULK (IFNγ-YFP x IL-10-GFP x FoxP3-RFP) donors and 1 × 10^6 BCR-ABL-NUP98hox9 leukemia cells. Recipients were untreated (haploBMT) or administered 50 mg/kg PT-Cy on D+3 and D+4 (PT-Cy) with or without decoy resistant IL-18 (PT-Cy + DR-18; 8μg twice weekly from D+7 to week 5) or CD137 agonist antibody (PT-Cy + αCD137; 100 μg twice weekly from D+7 to week 5). **(A)** Experimental design. **(B)** Number of GFP^+ leukemia cells in blood, leukemic death and overall median survival. **(C-J)** Mice

with <5% leukemia cells in BM were sacrificed at 21 days after transplantation and BM was analyzed (n = 4–5; 1 experiment). **(C)** Total numbers of $CD8^+$ T, $CD4^+$ T, and NK cells. **(D)** Percentage of IFNγ-producing $CD8^+$ and $CD4^+$ T cells. **(E)** Co-expression of DNAM-1 and TIGIT and **(F)** MFI on $CD8^+$ T cells. **(G)** Expression of TIM-3 and TOX on $CD8^+$ T cells. **(H)** Granzyme A and B expression in $CD8^+$ T cells. **(I)** IFNγ and **(J)** granzyme A and B production in NK cells. One-way ANOVA with Tukey's multiple comparisons test and Log-rank for survival. Data is mean ± SEM * $p<0.05$, ** $p<0.01$, *** $p<0.001$